

AN OPEN-ENDED BENCHMARK AND FORMAL FRAMEWORK FOR ADJUVANT RESEARCH WITH MLLMs

005 **Anonymous authors**

006 Paper under double-blind review

ABSTRACT

011 Adjuvants play a critical role in modulating immune responses and are central
 012 to the development of vaccines and immunotherapies. Yet progress in this field
 013 is constrained by data scarcity and incomplete understanding of mechanisms of
 014 action, which limit the transition from experience-based design to AI-driven ap-
 015 proaches. To address these challenges, we present the first benchmark dedicated to
 016 adjuvants, constructed in an open-ended Q&A format and annotated by domain
 017 experts. The benchmark comprises 1,294 Q&A pairs and 1,364 formal descriptions,
 018 providing a resource for evaluating general-purpose multimodal large language
 019 models (MLLMs) and for developing domain-specific systems. We systematically
 020 assess 11 closed-source and 18 open-source MLLMs across dimensions including
 021 domain-specific Q&A, hallucination rejection, data generation, and instruction
 022 following. Results indicate that OpenAI-o1 (STS = 0.7495, LLM Score = 7.7) and
 023 DeepSeek-R1 (STS = 0.7415, LLM Score = 7.7) achieved the strongest per-
 024 formance among closed- and open-source models, respectively. In addition, we
 025 introduce a formal description framework for representing adjuvant design prin-
 026 ciples and immune mechanisms as structured abstractions, which can serve as
 027 building blocks for future domain-specialized MLLMs. Overall, this work provides
 028 a first step toward systematically integrating MLLMs into adjuvant research by
 029 offering a dedicated benchmark, comparative evaluation of existing models, and
 030 a formal foundation for future development. Data and code will be released at
 031 Anonymous.

1 INTRODUCTION

032 Artificial intelligence (AI) has become an important driver of scientific discovery, offering new
 033 perspectives and tools to address increasingly complex challenges Hessler & Baringhaus (2018);
 034 Jumper et al. (2021); Xu et al. (2021); Esteva et al. (2019; 2021); Rajpurkar et al. (2022). Early
 035 applications in science often relied on task-specific datasets and bespoke neural architectures Krenn
 036 et al. (2020); Wu et al. (2018); Xie & Grossman (2018); de Teresa-Trueba et al. (2023), but recent
 037 advances in multimodal large language models (MLLMs) have shifted attention toward more general
 038 frameworks capable of integrating heterogeneous information sources Liu et al. (2023); Li et al.
 039 (2024); OpenAI (2023); Team et al. (2023). These models demonstrate broad capabilities in domains
 040 ranging from language and vision to biomedicine, enabling new paradigms for reasoning and analysis
 041 He et al. (2024); Xie et al. (2023); Outeiral & Deane (2024). Representative work includes LLaVA-
 042 Med, a vision-language assistant for biomedical images Li et al. (2023), and BiomedGPT, a generalist
 043 biomedical foundation model Zhang et al. (2024b).

044 Table 1: Cross-domain availability of datasets, methods, and mechanistic principles.

	Drug Discovery	Protein Structure	Genomics/Omics	Catalyst Design	Battery Materials	Adjuvants
Datasets	✓	✓	✓	✓	✓	✗
Methods	✓	✓	✓	✓	✓	✗
Principles	✓	✓	✓	✓	✓	✗

045 Adjuvants are indispensable components of modern vaccines, as they enhance immune responses,
 046 prolong protection, and in some cases determine whether a vaccine is clinically viable Glenny et al.
 047 (1926); Iwasaki & Omer (2020); Reed et al. (2013). They are particularly critical for emerging
 048 infectious diseases and cancer immunotherapy, where rapid and robust immune activation is essential.

Despite their importance, the field remains underserved by AI. As shown in Table 1, unlike drug discovery or protein structure prediction—where large-scale datasets and standardized benchmarks already exist—adjuvant research faces three persistent barriers: **(i)** limited systematically curated data, **(ii)** a lack of AI methodologies tailored to adjuvant knowledge, and **(iii)** heterogeneous definitions and mechanisms that complicate systematic modeling Guy (2007). As a result, existing biomedical benchmarks cannot be directly applied, and building domain-specific infrastructure is necessary for progress.

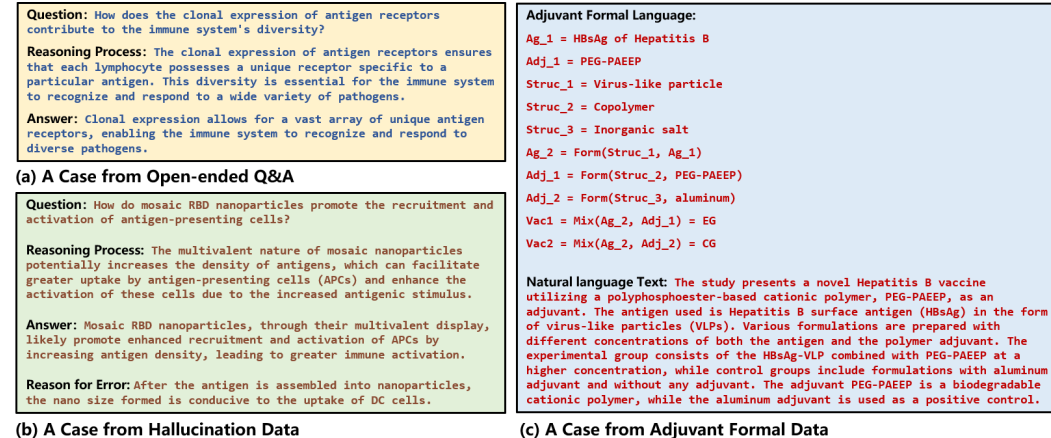


Figure 1: Three Types of Data Display in Adjuvant Benchmark

To address this gap, we present the first benchmark for adjuvants. We adopt an *open-ended Q&A format* to capture mechanistic reasoning, design considerations, and safety issues that cannot be represented through multiple-choice tasks. In parallel, we propose a formal description framework that translates complex biological intuitions into structured abstractions to support reasoning beyond retrieval. Concretely, we generated candidate data with four state-of-the-art MLLMs and conducted rigorous expert annotation across vaccine subdomains. The resulting benchmark consists of three components (Fig. 1): **Open-ended Q&A Data**, **Hallucination Data**, and **Adjuvant Formal Data**. We then evaluated 11 closed-source and 18 open-source MLLMs on these tasks, assessing domain-specific answering, hallucination rejection, and instruction following, and complemented these with expert-based subjective assessments of generation quality.

Our main contributions are summarized as follows:

- We establish the **first high-quality benchmark dedicated to adjuvants**, explicitly designed to fill a long-standing gap in biomedical AI benchmarks and to support subsequent MLLM research.
- We perform the first systematic evaluation of mainstream general-purpose MLLMs (**11 closed-source and 18 open-source**) on adjuvant knowledge, assessing critical capabilities including data generation, domain-specific QA, hallucination rejection, and prompt following. This provides initial conclusions on the capabilities and limitations of current models, and concrete guidance for selecting base models in this domain.
- We introduce **formal descriptions of adjuvants**, converting their complex biological mechanisms into simplified abstractions that can be directly used in training or reasoning. This approach lays the groundwork for future domain-specific MLLMs that combine statistical learning with symbolic reasoning.

2 RELATED WORK

2.1 ADJUVANTS

Adjuvants are crucial components that are used to improve the effectiveness of vaccines, primarily by stimulating the immune system to improve recognition and response to antigens. By increasing the potency of vaccines, they enable the immune system to respond more rapidly and effectively to pathogens Zhao et al. (2023). Adjuvants can encompass a diverse range of substances, including

108 synthetic small molecule compounds, complex natural extracts, and particulate materials, each
 109 contributing uniquely to the modulation of immune responses McKee et al. (2007).
 110

111 Despite the long-standing and increasing diversity of adjuvants used in vaccines, the mechanisms by
 112 which they enhance immune responses are not yet fully understood. With the elucidation of how the
 113 innate immune response regulates the adaptive immune response, researchers began to gain insight
 114 into the operational mechanisms of adjuvants Coffman et al. (2010). Although this work has provided
 115 a certain degree of elucidation regarding the modes of action of adjuvants, a systematic overview
 116 and summary of their mechanisms remain scarce due to the broad definition and complex nature of
 117 adjuvants.

118 Recent studies have begun to explore the integration of adjuvants with machine learning to optimize
 119 adjuvant selection, such as Nagpal et al. (2018) used the support vector machine (SVM) to develop a
 120 hybrid model for predicting A-cell epitopes, which enhances the identification of immune epitopes.
 121 Ma et al. (2023) utilized machine learning to identify molecular properties that target Toll-like
 122 receptors (TLRs) and designed two new adjuvants to enhance vaccine responses. These effectively
 123 promote strong immune responses, significantly suppressing tumor growth and metastases. Chaudhury
 124 et al. (2018). used random forest algorithms to develop a predictive model that achieves 92% accuracy
 125 in predicting adjuvant conditions based on immune response data, facilitating the identification of
 126 immune characteristics of different adjuvants and aiding in the rational pairing of vaccines and
 127 adjuvants.

128 However, these methods often lack generalizability, limiting their effectiveness in complex scenarios.
 129 In contrast, MLLMs can learn from vast and diverse modalities, identifying underlying patterns
 130 that traditional methods may overlook. This capability enables them to generate more accurate
 131 and efficient insights and predictions. By integrating MLLMs with adjuvant research, we aim to
 132 accelerate adjuvant development, provide a more responsive approach to public health emergencies,
 133 and shift the current paradigm from trial-and-error, experience-based methods to a more AI-driven
 134 and efficient process.

135 2.2 SCIENCE BENCHMARK

136 Recently, there has been increasing attention on MLLMs in scientific research. To evaluate and
 137 improve the performance of MLLMs in specific research domains, it is crucial to establish rigorous
 138 benchmarks. These not only help in assessing the accuracy and efficiency of the models but also
 139 ensure that the evaluation of different methodologies used is consistent and fair across the same
 140 studies.

141 Zhang et al. (2024a) developed ChemBench, an innovative chemical benchmark consisting of 4,100
 142 multiple-choice questions in nine tasks related to chemical molecules and reactions, aiming at ob-
 143 jectively measuring the chemical proficiency of large language models (LLMs). Chen et al. (2023)
 144 proposed an extensive benchmark study on biomedical text generation, which highlights the strengths
 145 and weaknesses of ChatGPT in addressing biomedical tasks, potentially inspiring further ad-
 146 vancements in NLP models for biomedical data analysis. Zhang et al. (2025) introduced DataSciBench, a
 147 novel and comprehensive benchmarking tool aimed at deeply evaluating the capabilities of LLMs
 148 in data science through natural and challenging tasks. He et al. (2023) proposed a system called
 149 SciGuard to control misuse risks associated with AI models in the field of science. They also intro-
 150 duced a red-teaming benchmark, SciMT-Safety, to assess the safety of different systems. Gao et al.
 151 (2025) proposed a model-level evaluation framework that emphasizes practical metrics aligned with
 152 real-world applications to address the limitations in structure-based drug design (SBDD).
 153

154 **Summary.** Despite the proliferation of benchmarks in domains like chemistry, biomedicine, and data
 155 science, none of them address the unique characteristics of adjuvant research. Existing biomedical
 156 benchmarks (e.g., PubMedQA Jin et al. (2019), ChemBench Walker et al. (2010)) mainly evaluate
 157 molecular properties, literature summarization, or general biomedical knowledge. In contrast,
 158 adjuvants involve heterogeneous substances, multi-scale immune mechanisms, and a lack of structured
 159 training data. This makes it impossible to directly apply existing benchmarks to this domain. Our
 160 work therefore, fills a critical gap by introducing the first dedicated benchmark for adjuvants, explicitly
 161 designed to capture mechanistic reasoning, safety evaluation, and design-oriented knowledge that are
 162 absent from prior benchmarks.

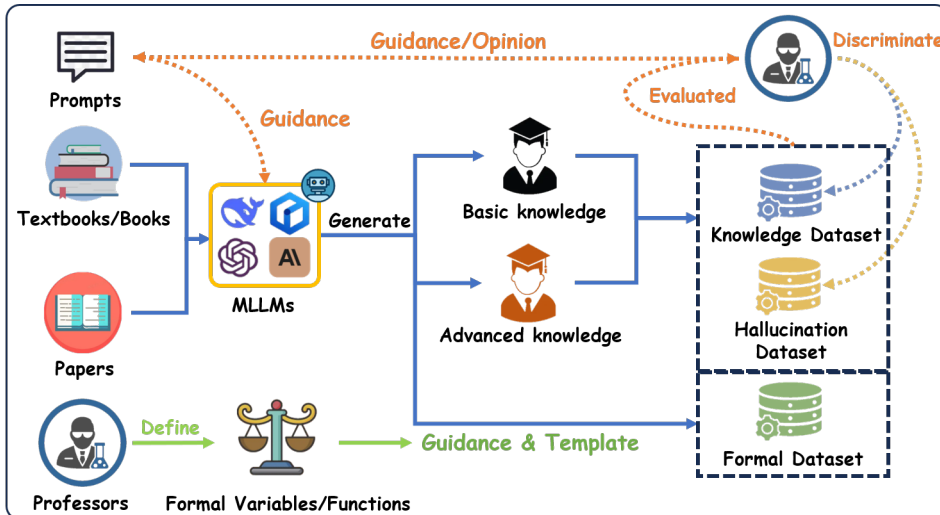
162 3 ADJUVANT BENCHMARK

164 3.1 OVERVIEW

166 Although immunology and adjuvant research have seen significant progress, the systematic integration
 167 of MLLMs into this field remains unexplored. To address this gap, we introduce the first benchmark
 168 explicitly designed for evaluating MLLMs on adjuvant-related knowledge and reasoning. By curating
 169 high-quality academic resources and leveraging multiple state-of-the-art MLLMs, we construct a
 170 domain-specific evaluation suite that captures both mechanistic understanding and practical design
 171 considerations. The following sections detail the benchmark construction pipeline, expert annotation
 172 process, and subsequent analyses of the resulting data.

173 3.2 PIPELINE OF BENCHMARK CONSTRUCTION

175 The overall construction pipeline is illustrated in Fig. 2. We first collected 739 peer-reviewed papers
 176 together with two classic textbooks, from which MLLMs automatically generated approximately 35k
 177 open-ended Q&A pairs on adjuvants and immunology, each accompanied by an explicit reasoning
 178 step (The generation prompts are described in Appendix G.1). To ensure quality and domain relevance,
 179 1.5k samples were randomly selected for expert review. After cleaning and careful labeling, 1,294
 180 high-quality Q&A pairs were retained as the meta dataset.



198 Figure 2: The Benchmark Construction Pipeline.

199 The annotation team consisted of 13 experts spanning infectious disease, cancer, and bacterial
 200 vaccines. All were trained under unified guidelines and evaluated each Q&A–reasoning triplet strictly
 201 against the source material. Items were labeled as either valid or hallucinated, with justifications
 202 provided for the latter. Detailed preprocessing and annotation workflows are described in Appendix B.

203 To reduce model-specific bias—particularly since the same system might otherwise generate and
 204 answer its own questions—we employed several MLLMs with long-context and multimodal support,
 205 including GPT-4o OpenAI, Claude3.5-Sonnet Claude, Ernie4.0-Turbo Baidu, and DeepSeek-R1 Guo
 206 et al. (2025).

207 Following expert annotation, the meta dataset was organized into three complementary components:
208 Open-ended Q&A Data, **209 Hallucination Data**, and **210 Adjuvant Formal Data**. Each component is
 211 described in detail in the subsequent sections.

212 3.3 STATISTICS OF BENCHMARK

213 3.3.1 OVERALL ANALYSIS

214 The overall distribution of the benchmark is shown in Fig. 3. Specifically, Fig. 3a illustrates the
 215 proportions of different data types, while Fig. 3b summarizes the contributions of various models

216 to Q&A generation. The benchmark is primarily composed of open-ended Q&A items and formal
 217 adjuvant data, with GPT-4o and DeepSeek-R1 contributing the majority of the high-quality entries.
 218 This reflects their comparatively stronger performance in preliminary generation and evaluation.
 219 Further details and representative examples are provided in Appendix A and Appendix G.

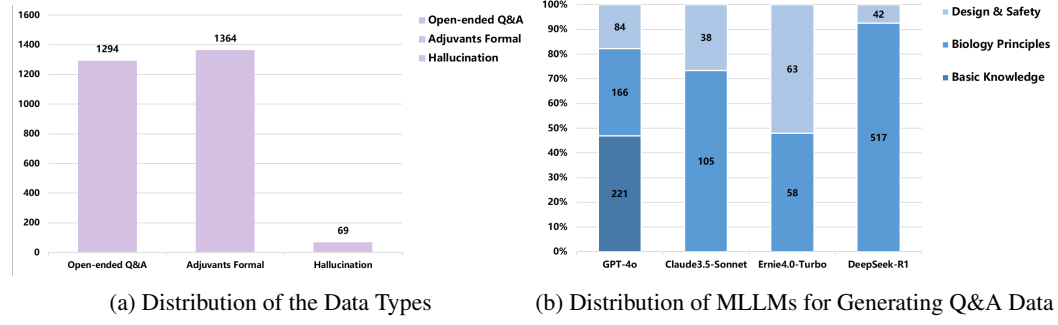


Figure 3: Distribution of the Adjuvant Benchmark

3.3.2 OPEN-ENDED Q&A DATA

The open-ended Q&A component is intended to evaluate the extent to which MLLMs capture adjuvant-related knowledge. It draws on both basic and advanced material curated from textbooks and peer-reviewed publications. The advanced category covers two major themes: *biological principles* (e.g., immunological mechanisms of adjuvant action) and *design & safety* (e.g., strategies for developing or modifying adjuvants and approaches for evaluating safety). Table 2 summarizes the distribution of these data, with the advanced subtypes highlighted.

Table 2: Distribution of Open-ended Q&A

Data Type	Basic Knowledge	Advanced Knowledge	Biology Principles	Design & Safety
Count	221	1073	846	227

Table 3: Hallucination Data

Data Type	Question	Answer	Overlap	Total
Hallucination	27	54	12	69

In addition, the benchmark includes multimodal content: 1,135 entries are text-only (87.7%), while 159 involve image-associated inputs (12.3%). This enables evaluation of both purely textual reasoning and multimodal understanding. Illustrative examples are provided in Appendix C.

3.3.3 HALLUCINATION DATA

In this study, the hallucination data follow the same structural format as the open-ended Q&A but differ in that the questions or answers have been reviewed by domain experts and explicitly judged to be incorrect. Rather than discarding these items, we retain them as a dedicated resource for evaluating the ability of MLLMs to recognize and reject hallucinations in the context of adjuvant and immunology tasks. For clarity, we distinguish two categories: *question hallucinations* and *answer hallucinations*. This dataset provides a controlled setting for analyzing the sources of hallucination errors and offers a reference point for the development of more reliable model evaluation and training strategies.

3.3.4 ADJUVANT FORMAL DATA

Formal descriptions are introduced to translate complex biological processes related to adjuvants into structured variables and functional transformations, with the aim of improving both the reasoning capacity and interpretability of MLLMs in this domain. Such formalized pathways also provide a systematic means of representing mechanisms that may otherwise remain implicit or fragmented in the literature.

To construct these descriptions, we worked with the same team of adjuvant experts described in Section 3.2 to design a set of formal variables and functions, thereby establishing expert-defined standards. These standards were organized into templates and incorporated into prompts for GPT-4o, which subsequently generated a total of **1,364** formal entries (Fig. 1c). The data are divided into two

270 balanced categories: *adjuvant design* and *adjuvant activation & immune processes*, each comprising
 271 **682** items. Detailed definitions of the variables and functions are provided in Appendix D.

272 Although this framework has not yet been applied to downstream model training, the released vari-
 273 ables and relationships—such as `Form(Struc, Ag)` and `Load(A, B, Surface)`—serve as
 274 structured building blocks for future adjuvant-specialized MLLMs. By providing a computable ab-
 275 straction of design principles and immune response processes, the framework establishes a foundation
 276 that can be extended in subsequent research.

278 4 EXPERIMENTS

281 4.1 EXPERIMENTAL SETTINGS

282 **MLLMs:** The set of evaluated models is listed in Table 4. Models highlighted in blue were also used
 283 in the data generation stage and were subsequently reviewed by adjuvant experts.

285 Table 4: Models evaluated on the adjuvant benchmark. Blue rows indicate models additionally used
 286 during data generation.

Model	#Size	Form	Ver.	Model	#Size	Form	Ver.
GPT-4o	N/A	api	latest	LLaVA1.5-13B	13B	open	v1.5
GPT-4.1	N/A	api	latest	Qwen2.5-VL-7B	7B	open	instruct
OpenAI-o1	N/A	api	latest	Qwen2.5-VL-72B	72B	open	instruct
Claude3.5	N/A	api	sonnet	Qwen3-8B	8B	open/api	think
Claude3.7	N/A	api	sonnet	Qwen3-32B	32B	open/api	think
Gemini1.5-Pro	N/A	api	latest	Qwen3-30B-A3B	30B	open/api	think
Gemini2.0-Pro	N/A	api	flash	Qwen3-235B-A22B	235B	open/api	think
Gemini2.5-Pro	N/A	api	flash	Internvl2.5-8B	8B	open	v2.5
Ernie3.5	N/A	api	latest	Internvl2.5-78B	78B	open	v2.5
Ernie4.0	N/A	api	turbo	Internvl3.0-8B	8B	open	v3.0
Doubaol1.5-Pro	N/A	api	250115	Internvl3.0-72B	72B	open	v3.0
DeepSeek-R1	671B	open/api	reasoner	InstructBlip-13B	13B	open	vicuna
DeepSeek-V3	671B	open/api	chat	Idefics-9B	9B	open	instruct
LLaVA1.5-7B	7B	open	v1.5	Darwin	7B	open	v1.5

299 **Inference:** Closed-source models were accessed through their official APIs. For open-source models,
 300 inference was performed with the official implementations on $8 \times$ NVIDIA A800 GPUs, following
 301 recommended hyperparameter settings. To ensure comparability across models, all were evaluated
 302 under identical prompts in a zero-shot setting (see Appendix G.2 for prompt details). To ensure
 303 fairness, regardless of whether the model supports multimodal input, we utilized a unified OCR engine
 304 to process the images and concatenated the OCR output with the original input text. Furthermore, we
 305 assessed the performance of the top 5 multimodal models on the image-related subset, with detailed
 306 experimental results provided in Appendix F.

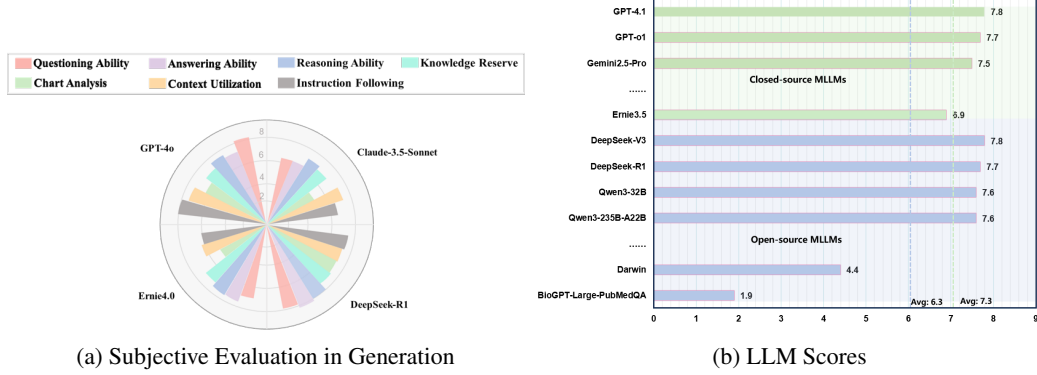
307 **Evaluation metrics:** To assess knowledge comprehension in the adjuvant domain, we employed a
 308 combination of automatic metrics and model-based scoring. Standard measures included Semantic
 309 Textual Similarity (STS) and BERTScore. In addition, we introduced an LLM-based rubric,
 310 implemented with GPT-4o and DeepSeek-R1, which scored answers along three axes: Similarity
 311 Score (SS), Scientific Rationality Score (RS), and Inclusiveness Score (IS), each on a 0–10 scale.
 312 This approach provides a scalable and reproducible way to evaluate factual accuracy and conceptual
 313 soundness, while reducing dependence on manual annotation. To further probe robustness, we report
 314 a Hallucination Rejection Ratio (HRR), which quantifies the ability of models to detect and avoid
 315 incorrect content. Detailed metric formulations are given in Appendix E.

316 4.2 EVALUATION OF GENERATION

318 During the annotation process, experts assigned subjective scores (0–10) to six dimensions: Ques-
 319 tioning Ability, Answering Ability, Reasoning Ability, Knowledge Reserve, Chart Analysis, Context
 320 Utilization, and Instruction Following. These scores reflect the overall quality and reliability of the
 321 generated content.

323 The results are summarized in Fig. 4a. DeepSeek-R1 obtained comparatively higher scores in both
 324 questioning and answering ability, indicating that it can produce relevant prompts and generate

324 responses with coherent reasoning in the adjuvant domain. GPT-4o achieved the highest score in
 325 questioning ability and also performed well in instruction following, suggesting that it is effective at
 326 generating focused inquiries and adhering to task specifications. In addition, GPT-4o showed broad
 327 coverage of domain knowledge, contributing to more comprehensive responses.



(a) Subjective Evaluation in Generation

(b) LLM Scores

Figure 4: Comprehensive Evaluation of MLLMs on the Adjuvant Benchmark

341 By contrast, Ernie4.0 and Claude3.5 received consistently lower scores across several categories,
 342 suggesting limitations in handling complex material from adjuvant-related literature.

343 Overall, the expert assessments highlight GPT-4o and DeepSeek-R1 as the strongest performers
 344 within this evaluation setting, particularly in tasks requiring both domain-specific questioning and
 345 reasoned answering. These findings provide a basis for selecting suitable base models for future work
 346 in adjuvant-focused applications.

349 4.3 EVALUATION OF ADJUVANT OPEN-ENDED Q&A

351 We evaluated 11 closed-source and 18 open-source MLLMs on the adjuvant open-ended Q&A task.
 352 Results are reported in Table 5, with blue highlighting used to indicate models achieving state-of-the-
 353 art performance under the given metrics. A comparison between closed- and open-source models is
 354 summarized below.

355 **Closed-source vs. Open-source:** On average, closed-source models achieved higher overall perfor-
 356 mance, with a mean LLM Score of 7.3 and an STS score of 0.7263, compared to 6.2 and 0.6846 for
 357 open-source models. Nevertheless, several open-source models exceeded the closed-source averages.
 358 DeepSeek-R1 (LLM Score = 7.7, STS = 0.7415), DeepSeek-V3 (LLM Score = 7.8, STS = 0.7289),
 359 Qwen3-23B (LLM Score = 7.6, STS = 0.7331), and Qwen3-32B (LLM Score = 7.6, STS = 0.7259)
 360 performed comparably to the strongest closed-source models, particularly in scientific rationality
 361 and inclusiveness. However, in terminology consistency, reflected by BERTScore, open-source
 362 models averaged 0.550, which remains below the closed-source average of 0.566. This suggests that
 363 while optimization strategies enable some open-source models to close the gap, challenges remain
 364 in aligning with domain-specific vocabulary. Overall, the observed performance differences appear
 365 to relate more to the extent of domain knowledge integration than to the proprietary or open-source
 366 nature of the models.

367 **Inference Models vs. Think Models:** Think-oriented models obtained higher scores in Rationality
 368 Score (RS), Inclusiveness Score (IS), and STS compared to inference-style models. This pattern
 369 suggests that their explicit reasoning mechanisms—such as multi-step causal decomposition and
 370 logical verification—contribute to producing more logically consistent and comprehensive answers.
 371 At the same time, the reliance on explicit reasoning chains increases decoding complexity, which may
 372 constrain efficiency in resource-limited settings. These observations indicate that combining explicit
 373 reasoning strategies with domain knowledge and structured representations could be a promising
 374 direction for future model development.

375 **Closed-source Models:** OpenAI-o1 (LLM Score = 7.7, STS = 0.7495) was the best-performing
 376 closed-source model in our setting. By contrast, Ernie4.0 (LLM Score = 6.9) and Doubao1.5-Pro
 377 (LLM Score = 7.1) obtained lower scores within this cohort. While performance differences may
 378 correlate with factors such as data coverage, training procedures, and model scale, the proprietary

378 nature of these systems prevents attributing causality from our evaluation alone. Closed-source
 379 models also pose practical constraints for scientific use, including limited transparency and higher
 380 inference costs, which may hinder broad adoption in open research workflows. Future work could
 381 explore more transparent and collaborative evaluation practices to facilitate integration into scientific
 382 pipelines.

Table 5: Evaluation Result of Adjuvants Open-ended Q&A

Model Category	STS Score	BertScore	LLM Score (GPT-4o)			LLM Score (DeepSeek-R1)			LLM Score Avg	
			SS	RS	IS	SS	RS	IS		
	Closed-source MLLMs									
<i>Inference Models</i>										
GPT-4o OpenAI	0.7261	0.5732	6.4	8.3	6.8	6.9	8.6	6.8	7.3	
GPT-4.1 OpenAI	0.7178	0.5420	7.0	8.5	7.2	7.6	9.0	7.6	7.8	
Claude3.5 Claude	0.7256	0.5750	6.2	8.2	6.7	6.8	8.7	6.9	7.3	
Claude3.7 Claude	0.7396	0.5650	6.5	8.2	6.8	7.0	8.7	7.1	7.4	
Gemini1.5-Pro Team et al. (2024)	0.7235	0.5644	6.3	8.2	6.7	6.9	8.8	7.1	7.3	
Gemini2.0-Pro Google	0.7118	0.5486	6.3	8.2	6.7	6.9	8.7	7.1	7.3	
Gemini2.5-Pro Google	0.7316	0.5664	6.6	8.4	7.0	7.2	8.9	7.1	7.5	
Ernie3.5 Baidu	0.7199	0.5554	6.1	8.0	6.5	6.4	8.2	6.2	6.9	
Ernie4.0 Baidu	0.7238	0.5587	6.0	8.0	6.4	6.4	8.2	6.2	6.9	
Doubaol1.5-Pro Volcengine	0.7201	0.5532	6.1	8.0	6.4	6.8	8.5	6.7	7.1	
<i>Think Models</i>										
OpenAI-o1 OpenAI	0.7495	0.6195	6.9	8.5	7.1	7.3	8.9	7.2	7.7	
Average	0.7263	0.5656	6.4	8.2	6.8	6.9	8.7	6.9	7.3	
<i>Open-source MLLMs</i>										
<i>Inference Models</i>										
DeepSeek-V3 Liu et al. (2024a)	0.7289	0.5276	6.8	8.4	7.0	7.6	9.0	7.7	7.8	
LLaVA1.5-7B Liu et al. (2024b)	0.7134	0.5823	5.2	7.0	5.2	5.3	6.7	4.6	5.7	
LLaVA1.5-13B Liu et al. (2024b)	0.7116	0.5838	5.4	7.1	5.4	5.4	6.9	4.8	5.8	
Qwen2.5-VL-7B Bai et al. (2025)	0.7151	0.5602	5.8	7.8	6.1	5.9	7.7	5.7	6.5	
Qwen2.5-VL-72B Bai et al. (2025)	0.7217	0.5649	6.2	8.2	6.7	6.6	8.4	6.5	7.1	
Internv1.2.5-8B Chen et al. (2024)	0.7217	0.5649	5.2	7.0	5.5	5.4	6.8	5.0	5.8	
Internv1.2.5-78B Chen et al. (2024)	0.6966	0.5606	6.0	7.8	6.3	6.2	7.9	6.0	6.7	
Internv1.3-0.8B Zhu et al. (2025)	0.6987	0.5526	5.6	7.6	6.0	6.0	7.6	5.9	6.5	
Internv1.3-0.78B Zhu et al. (2025)	0.7173	0.5608	6.2	8.1	6.6	6.6	8.3	6.5	7.1	
InstructBlip-13B Dai et al. (2023)	0.5960	0.5551	4.9	6.2	4.5	5.0	6.3	4.3	5.2	
Idefics-9B Laurencon et al. (2023)	0.5662	0.4718	4.5	6.2	4.3	4.8	6.1	4.2	5.0	
<i>Think Models</i>										
DeepSeek-R1 Guo et al. (2025)	0.7415	0.5485	6.6	8.4	7.1	7.5	9.0	7.7	7.7	
Qwen3.8B Bai et al. (2025)	0.7275	0.5387	6.5	8.1	6.7	7.1	8.6	7.2	7.4	
Qwen3.32B Bai et al. (2025)	0.7259	0.5371	6.6	8.1	6.9	7.3	8.8	7.6	7.6	
Qwen3.30B-A3B Bai et al. (2025)	0.7262	0.5411	6.5	8.3	6.9	7.2	8.8	7.3	7.5	
Qwen3.235B-A22B Bai et al. (2025)	0.7331	0.5497	6.5	8.4	7.0	7.3	8.9	7.6	7.6	
<i>Domain-Specific Models</i>										
Darwin Xie et al. (2025b)	0.6376	0.6245	4.4	5.5	3.8	4.1	5.4	3.1	4.4	
BioGPT-Large-PubMedQA Luo et al. (2022)	0.5468	0.4906	1.7	2.3	1.3	1.9	2.5	1.7	1.9	
Average	0.6904	0.5509	5.6	7.3	5.7	5.9	7.4	5.7	6.3	

408 **Open-source Models:** Among the open-source systems, DeepSeek-V3 achieved the highest overall
 409 performance. DeepSeek-R1 (LLM Score = 7.7), Qwen3-32B (LLM Score = 7.6), and Qwen3-235B
 410 (LLM Score = 7.6) all surpassed the closed-source average (7.3). These models employed explicit
 411 reasoning strategies, such as causal decomposition and multi-step verification, which contributed to
 412 higher scientific rationality scores and in some cases exceeded those of closed-source models (e.g.,
 413 Claude3.5). This suggests that open-source models can exhibit strong logical reasoning capabilities,
 414 although they often rely on decomposition and iterative reasoning to mitigate limitations in domain-
 415 specific knowledge.

416 DeepSeek-R1 and Qwen3-235B also incorporate Mixture of Experts (MoE) architectures, where
 417 dynamic expert routing enables finer-grained knowledge integration. While MoE contributes to
 418 improvements in reasoning and task decomposition, terminology consistency remains a challenge:
 419 BERTScore for these models is still lower than that of closed-source models such as GPT-4o. This
 420 indicates that MoE and reinforcement learning approaches alone are insufficient, and domain-adaptive
 421 pretraining remains necessary for accurate use of specialized terminology.

422 An additional observation is the non-linear relationship between parameter scale and performance:
 423 Qwen3-235B and Qwen3-32B achieved similar LLM Score despite their large difference in size. This
 424 pattern highlights diminishing returns from scaling alone and underscores the importance of targeted
 425 knowledge injection for domain adaptation. By contrast, models such as InstructBlip-13B and
 426 Idefics-9B underperformed across most metrics, reflecting architectural and training-data limitations
 427 in earlier generations of multimodal LLMs.

428 **Domain-Specific Models:** The comparatively lower performance of domain-specific biomedical
 429 and materials models indicates limitations in directly transferring such architectures to adjuvant
 430 tasks. Their training objectives, often centered on literature summarization or general biomedical
 431 QA, are not well aligned with the requirements of adjuvant-focused Q&A, leading to weaker answer
 432 quality (see Appendix F.4 for detailed examples). These results reinforce the view that progress

in adjuvant research requires purpose-built datasets rather than relying solely on fine-tuning with broader biomedical or materials corpora. Notably, the Darwin model obtained the highest BERTScore among all models, which may be linked to its use of open-ended Q&A data during initial training, partially aligning it with the evaluation setting.

Overall, models from the GPT, DeepSeek, and Qwen3.0 families demonstrated relatively strong performance across multiple metrics, suggesting that these families already possess the capacity to contribute as auxiliary tools for basic research and as potential foundations for future adjuvant-specialized systems.

4.4 EVALUATION OF HALLUCINATION REJECTION

We evaluated the top five models (both closed-source and open-source) based on their LLM Scores for their ability to reject hallucinations. Results are reported in Table 6.

Table 6: Evaluation of Hallucination Rejection Capabilities (Mean \pm SD over 10 shuffled evaluation)

Model Category	Question HRR (%)	Answer HRR (%)	Overall HRR (%)
GPT-4o	30.74% (\pm 4.95%)	23.33% (\pm 2.92%)	26.23% (\pm 2.85%)
GPT-4.1	22.22% (\pm 2.47%)	14.26% (\pm 1.25%)	17.10% (\pm 1.14%)
OpenAI-o1	24.07% (\pm 4.70%)	18.15% (\pm 2.10%)	20.58% (\pm 2.72%)
Gemini 2.5 Pro	18.15% (\pm 3.68%)	9.07% (\pm 1.84%)	12.32% (\pm 1.41%)
Claude3.7	13.33% (\pm 2.59%)	22.96% (\pm 1.79%)	21.59% (\pm 1.59%)
DeepSeek-V3	0.00% (\pm 0.00%)	2.69% (\pm 0.92%)	2.10% (\pm 0.72%)
DeepSeek-R1	22.59% (\pm 4.08%)	12.04% (\pm 3.18%)	16.23% (\pm 3.19%)
Qwen3-8B	12.96% (\pm 4.70%)	10.37% (\pm 1.79%)	11.74% (\pm 1.74%)
Qwen3-32B	14.81% (\pm 3.49%)	8.52% (\pm 3.17%)	8.52% (\pm 3.17%)
Qwen3-30B-A3B	21.11% (\pm 5.25%)	17.22% (\pm 1.96%)	18.99% (\pm 2.41%)
Qwen3-235B-A22B	23.33% (\pm 6.06%)	16.15% (\pm 3.53%)	18.73% (\pm 3.13%)

Both closed- and open-source models exhibited limited capability in hallucination rejection. The median HRR for closed-source models was 20.58%, compared to 13.99% for open-source models, which falls below the level generally required for reliable application in practice. For example, DeepSeek-V3 performed strongly on the adjuvant Q&A task (LLM Score = 7.8) but obtained the lowest HRR (2.10%), highlighting the inconsistency between knowledge answering and hallucination rejection.

These findings suggest that current models often rely on surface-level language correlations rather than deeper domain reasoning, which constrains their ability to identify and reject incorrect content. Improving hallucination control in this setting will likely require domain-adaptive fine-tuning combined with structured knowledge representations, in order to enhance logical coherence and scientific reliability. Additional analyses are provided in Appendix F.

5 CONCLUSIONS AND LIMITATIONS

This work presents the first benchmark dedicated to adjuvants, combining 1,294 expert-annotated Q&A pairs and 1,364 formal descriptions. Using this resource, we systematically evaluated 11 closed-source and 18 open-source MLLMs across open-ended Q&A, hallucination rejection, and instruction following. Our results highlight comparatively strong performance from the GPT, DeepSeek-R1, and Qwen3.0 families, and we propose a formal framework that abstracts adjuvant design principles and immune mechanisms into structured representations to support future domain-specific models.

While our study provides an initial foundation, further progress will require stratified benchmarks to capture varying task difficulty, domain-adaptive training for expert knowledge integration, and hybrid neuro-symbolic architectures that leverage the proposed formal framework. Beyond technical evaluation, the benchmark and formal abstractions may lower the entry barrier for applying MLLMs in immunology and help systematize reasoning in vaccine adjuvant research. These resources are intended solely for research purposes and should not be used directly in clinical contexts without expert validation.

486
487
ETHICS STATEMENT488
489
This paper adheres to the ICLR Code of Ethics. We acknowledge that our research follows ethical
490
guidelines, ensuring compliance with all relevant regulations.491
492
• **Human Subjects:** No human subjects were involved in this research. All data used in the
493
study are publicly available datasets or generated synthetically.
494
• **Data Privacy and Security:** We have taken care to ensure that all data used complies with
495
relevant data protection laws. Datasets used in this research do not contain any personal,
496
confidential, or sensitive information.
497
• **Research Integrity:** We confirm that the research presented is original and has not been
498
plagiarized. All sources and data are properly cited and documented.
499
• **Legal Compliance:** We confirm that the research complies with all applicable laws and
500
ethical standards, including data usage and research practices.501
502
This statement is meant to address potential concerns in accordance with the ICLR Code of Ethics.
503504
505
REPRODUCIBILITY STATEMENT506
507
We ensure that our work is reproducible by providing all necessary resources for others to replicate
508
our experiments. Specifically:509
510
• **Benchmark Data and Experimental Setup:** All datasets used in the experiments, along
511
with detailed data processing steps, are publicly available. The experimental setup is also
512
provided, including hyperparameters, evaluation metrics, and the benchmarking environment.
513
• **Source Code:** The code used to process the data and conduct the benchmarking experiments
514
is available in an anonymous repository. This includes all scripts necessary for replicating
515
the experiments as described in the paper.516
517
By providing these resources, we aim to make our results fully reproducible and facilitate further
518
research based on our work. The details required for reproduction can be found in the anonymous
519
repository.520
521
REFERENCES522
523
Shuai Bai, Keqin Chen, Xuejing Liu, Jialin Wang, Wenbin Ge, Sibo Song, Kai Dang, Peng Wang,
524
Shijie Wang, Jun Tang, Humen Zhong, Yuanzhi Zhu, Mingkun Yang, Zhaohai Li, Jianqiang Wan,
525
Pengfei Wang, Wei Ding, Zheren Fu, Yiheng Xu, Jiabo Ye, Xi Zhang, Tianbao Xie, Zesen Cheng,
526
Hang Zhang, Zhibo Yang, Haiyang Xu, and Junyang Lin. Qwen2.5-vl technical report. *ArXiv*
527
preprint ArXiv:2502.13923, 2025.528
529
Baidu. Available online: <https://yidian.baidu.com/>. Accessed on 17 October 2023.530
531
Iz Beltagy, Kyle Lo, and Arman Cohan. Scibert: A pretrained language model for scientific text.
532
In *Proceedings of the 2019 Conference on Empirical Methods in Natural Language Processing*.
533
Association for Computational Linguistics, 2019. URL <https://www.aclweb.org/anthology/D19-1371>.534
535
Sidhartha Chaudhury, Elizabeth H Duncan, Tanmaya Atre, Casey K Storme, Kevin Beck, Stephen A
536
Kaba, David E Lanar, and Elke S Bergmann-Leitner. Identification of immune signatures of novel
537
adjuvant formulations using machine learning. *Scientific Reports*, 8(1):17508, 2018.538
539
Qijie Chen, Haotong Sun, Haoyang Liu, Yinghui Jiang, Ting Ran, Xurui Jin, Xianglu Xiao, Zhimin
Lin, Hongming Chen, and Zhangmin Niu. An extensive benchmark study on biomedical text
generation and mining with chatgpt. *Bioinformatics*, 39(9):btad557, 2023.

540 Zhe Chen, Jiannan Wu, Wenhai Wang, Weijie Su, Guo Chen, Sen Xing, Muyan Zhong, Qinglong
 541 Zhang, Xizhou Zhu, Lewei Lu, et al. Internvl: Scaling up vision foundation models and aligning
 542 for generic visual-linguistic tasks. In *Proceedings of the IEEE/CVF Conference on Computer
 543 Vision and Pattern Recognition*, pp. 24185–24198, 2024.

544 Claude. Available from: <https://www.anthropic.com/clause>. Accessed 27 Jun 2024.

545 Robert L Coffman, Alan Sher, and Robert A Seder. Vaccine adjuvants: putting innate immunity to
 546 work. *Immunity*, 33(4):492–503, 2010.

547 Wenliang Dai, Junnan Li, Dongxu Li, Anthony Meng Huat Tiong, Junqi Zhao, Weisheng Wang,
 548 Boyang Li, Pascale Fung, and Steven Hoi. Instructblip: Towards general-purpose vision-language
 549 models with instruction tuning. *ArXiv preprint ArXiv:2305.06500*, 2023.

550 Irene de Teresa-Trueba, Sara K Goetz, Alexander Mattausch, Frosina Stojanovska, Christian E
 551 Zimmerli, Mauricio Toro-Nahuelpán, Dorothy WC Cheng, Fergus Tollervey, Constantin Pape,
 552 Martin Beck, et al. Convolutional networks for supervised mining of molecular patterns within
 553 cellular context. *Nature Methods*, 20(2):284–294, 2023.

554 Jennifer D’Souza, Hamed Babaei Giglou, and Quentin Münch. Yescieval: Robust llm-as-a-judge for
 555 scientific question answering. *arXiv preprint arXiv:2505.14279*, 2025.

556 Yann Dubois, Percy Liang, and Tatsunori Hashimoto. Length-controlled alpacaeval: A simple
 557 debiasing of automatic evaluators. In *First Conference on Language Modeling*, 2024.

558 Andre Esteva, Alexandre Robicquet, Bharath Ramsundar, Volodymyr Kuleshov, Mark DePristo,
 559 Katherine Chou, Claire Cui, Greg Corrado, Sebastian Thrun, and Jeff Dean. A guide to deep
 560 learning in healthcare. *Nature Medicine*, 25(1):24–29, 2019.

561 Andre Esteva, Katherine Chou, Serena Yeung, Nikhil Naik, Ali Madani, Ali Mottaghi, Yun Liu, Eric
 562 Topol, Jeff Dean, and Richard Socher. Deep learning-enabled medical computer vision. *NPJ
 563 Digital Medicine*, 4(1):5, 2021.

564 Bowen Gao, Haichuan Tan, Yanwen Huang, Minsi Ren, Xiao Huang, Wei-Ying Ma, Ya-Qin Zhang,
 565 and Yanyan Lan. Reframing structure-based drug design model evaluation via metrics correlated
 566 to practical needs. In *The Thirteenth International Conference on Learning Representations*, 2025.
 567 URL <https://openreview.net/forum?id=RyWypcIMiE>.

568 AT Glenny, CG Pope, Hilda Waddington, and U Wallace. Immunological notes. xvii–xxiv. *J. Pathol.
 569 Bacteriol*, 29(1):31–40, 1926.

570 Google. Available online: <https://deepmind.google/technologies/gemini/>.

571 Daya Guo, Dejian Yang, Huawei Zhang, Junxiao Song, Ruoyu Zhang, Runxin Xu, Qihao Zhu,
 572 Shirong Ma, Peiyi Wang, Xiao Bi, et al. Deepseek-r1: Incentivizing reasoning capability in llms
 573 via reinforcement learning. *ArXiv preprint ArXiv:2501.12948*, 2025.

574 Bruno Guy. The perfect mix: recent progress in adjuvant research. *Nature Reviews Microbiology*, 5
 575 (7):396–397, 2007.

576 Jiyan He, Weitao Feng, Yaosen Min, Jingwei Yi, Kunsheng Tang, Shuai Li, Jie Zhang, Kejiang Chen,
 577 Wenbo Zhou, Xing Xie, et al. Control risk for potential misuse of artificial intelligence in science.
 578 *ArXiv preprint ArXiv:2312.06632*, 2023.

579 Yong He, Pan Fang, Yongtao Shan, Yuanfei Pan, Yanhong Wei, Yichang Chen, Yihao Chen, Yi Liu,
 580 Zhenyu Zeng, Zhan Zhou, et al. Lucaone: generalized biological foundation model with unified
 581 nucleic acid and protein language. *BioRxiv*, pp. 2024–05, 2024.

582 Gerhard Hessler and Karl-Heinz Beringhaus. Artificial intelligence in drug design. *Molecules*, 23
 583 (10):2520, 2018.

584 Akiko Iwasaki and Saad B Omer. Why and how vaccines work. *Cell*, 183(2):290–295, 2020.

594 Qiao Jin, Bhuwan Dhingra, Zhengping Liu, William Cohen, and Xinghua Lu. Pubmedqa: A dataset
 595 for biomedical research question answering. In *Proceedings of the 2019 Conference on Empirical
 596 Methods in Natural Language Processing and the 9th International Joint Conference on Natural
 597 Language Processing (EMNLP-IJCNLP)*, pp. 2567–2577, 2019.

598 John Jumper, Richard Evans, Alexander Pritzel, Tim Green, Michael Figurnov, Olaf Ronneberger,
 599 Kathryn Tunyasuvunakool, Russ Bates, Augustin Žídek, Anna Potapenko, et al. Highly accurate
 600 protein structure prediction with AlphaFold. *Nature*, 596(7873):583–589, 2021.

602 Seungone Kim, Jamin Shin, Yejin Cho, Joel Jang, Shayne Longpre, Hwaran Lee, Sangdoo Yun,
 603 Seongjin Shin, Sungdong Kim, James Thorne, and Minjoon Seo. Prometheus: Inducing
 604 fine-grained evaluation capability in language models. In *The Twelfth International Conference
 605 on Learning Representations*, 2024. URL <https://openreview.net/forum?id=8euJaTveKw>.

607 Mario Krenn, Florian Häse, Akshat Kumar Nigam, Pascal Friederich, and Alán Aspuru-Guzik. Self-
 608 referencing embedded strings (selfies): A 100% robust molecular string representation. *Machine
 609 Learning: Science and Technology*, 1(4):045024, 2020.

610 Md Tahmid Rahman Laskar, Israt Jahan, Elham Dolatabadi, Chun Peng, Enamul Hoque, and Jimmy
 611 Huang. Improving automatic evaluation of large language models (llms) in biomedical relation
 612 extraction via llms-as-the-judge. *arXiv preprint arXiv:2506.00777*, 2025.

614 Hugo Laurençon, Lucile Saulnier, Léo Tronchon, Stas Bekman, Amanpreet Singh, Anton Lozhkov,
 615 Thomas Wang, Siddharth Karamchetti, Alexander M. Rush, Douwe Kiela, Matthieu Cord, and
 616 Victor Sanh. Obelics: An open web-scale filtered dataset of interleaved image-text documents.
 617 *ArXiv preprint ArXiv:2306.16527*, 2023.

618 Chunyuan Li, Cliff Wong, Sheng Zhang, Naoto Usuyama, Haotian Liu, Jianwei Yang, Tristan
 619 Naumann, Hoifung Poon, and Jianfeng Gao. Llava-med: Training a large language-and-vision
 620 assistant for biomedicine in one day. *Advances in Neural Information Processing Systems*, 36:
 621 28541–28564, 2023.

623 Feng Li, Renrui Zhang, Hao Zhang, Yuanhan Zhang, Bo Li, Wei Li, Zejun Ma, and Chunyuan Li.
 624 Llava-next-interleave: Tackling multi-image, video, and 3d in large multimodal models. *ArXiv
 625 preprint ArXiv:2407.07895*, 2024.

626 Aixin Liu, Bei Feng, Bing Xue, Bingxuan Wang, Bochao Wu, Chengda Lu, Chenggang Zhao,
 627 Chengqi Deng, Chenyu Zhang, Chong Ruan, et al. Deepseek-v3 technical report. *ArXiv preprint
 628 ArXiv:2412.19437*, 2024a.

630 Haotian Liu, Chunyuan Li, Yuheng Li, and Yong Jae Lee. Improved baselines with visual instruction
 631 tuning. In *NeurIPS 2023 Workshop on Instruction Tuning and Instruction Following*, 2023.

632 Haotian Liu, Chunyuan Li, Qingyang Wu, and Yong Jae Lee. Visual instruction tuning. *Advances in
 633 Neural Information Processing Systems*, 36, 2024b.

635 Renqian Luo, Lai Sun, Yingce Xia, Tao Qin, Sheng Zhang, Hoifung Poon, and Tie-Yan Liu.
 636 Biogpt: generative pre-trained transformer for biomedical text generation and mining. *Briefings in
 637 Bioinformatics*, 23(6):bbac409, 2022.

638 Juan Ma, Shenqing Wang, Chuanfang Zhao, Xiliang Yan, Quanzhong Ren, Zheng Dong, Jiahuang
 639 Qiu, Yin Liu, Qing'e Shan, Ming Xu, et al. Computer-aided discovery of potent broad-spectrum
 640 vaccine adjuvants. *Angewandte Chemie International Edition*, 62(18):e202301059, 2023.

642 Amy S McKee, Michael W Munks, and Philippa Marrack. How do adjuvants work? important
 643 considerations for new generation adjuvants. *Immunity*, 27(5):687–690, 2007.

644 Gandharva Nagpal, Kumardeep Chaudhary, Piyush Agrawal, and Gajendra PS Raghava. Computer-
 645 aided prediction of antigen presenting cell modulators for designing peptide-based vaccine adju-
 646 vants. *Journal of Translational Medicine*, 16:1–15, 2018.

647 OpenAI. Available online: <https://openai.com/index/>. Accessed on 29 May 2024.

648 OpenAI. Gpt-4v (ision) system card. *Citekey: gptvision*, 2023.
 649

650 Carlos Outeiral and Charlotte M Deane. Perfecting antibodies with language models. *nature
 651 Biotechnology*, 42(2):185–186, 2024.

652 Arjun Panickssery, Samuel Bowman, and Shi Feng. Llm evaluators recognize and favor their own
 653 generations. *Advances in Neural Information Processing Systems*, 37:68772–68802, 2024.

654

655 Pranav Rajpurkar, Emma Chen, Oishi Banerjee, and Eric J Topol. AI in health and medicine. *Nature
 656 Medicine*, 28(1):31–38, 2022.

657

658 Steven G Reed, Mark T Orr, and Christopher B Fox. Key roles of adjuvants in modern vaccines.
 659 *Nature Medicine*, 19(12):1597–1608, 2013.

660 Nils Reimers and Iryna Gurevych. Sentence-bert: Sentence embeddings using siamese bert-networks.
 661 In *Proceedings of the 2019 Conference on Empirical Methods in Natural Language Processing*.
 662 Association for Computational Linguistics, 11 2019. URL <https://ArXiv.org/abs/1908.10084>.

663

664 Andreas Stephan, Dawei Zhu, Matthias Aßenmacher, Xiaoyu Shen, and Benjamin Roth. From
 665 calculation to adjudication: Examining llm judges on mathematical reasoning tasks. *arXiv preprint
 666 arXiv:2409.04168*, 2024.

667

668 Gemini Team, Rohan Anil, Sebastian Borgeaud, Yonghui Wu, Jean-Baptiste Alayrac, Jiahui Yu, Radu
 669 Soricut, Johan Schalkwyk, Andrew M Dai, Anja Hauth, et al. Gemini: a family of highly capable
 670 multimodal models. *ArXiv preprint ArXiv:2312.11805*, 2023.

671

672 Gemini Team, Petko Georgiev, Ving Ian Lei, Ryan Burnell, Libin Bai, Anmol Gulati, Garrett
 673 Tanzer, Damien Vincent, Zhufeng Pan, Shibo Wang, et al. Gemini 1.5: Unlocking multimodal
 674 understanding across millions of tokens of context. *ArXiv preprint ArXiv:2403.05530*, 2024.

675

676 Volcengine. Available online: <https://www.volcengine.com/product/doubao>. Ac-
 677 cessed on 18 December 2024.

678

679 Theo Walker, Christopher M Grulke, Diane Pozefsky, and Alexander Tropsha. Chembench: a
 680 cheminformatics workbench. *Bioinformatics*, 26(23):3000–3001, 2010.

681

682 Haoyuan Wang, Rui Yang, Mahmoud Alwakeel, Ankit Kayastha, Anand Chowdhury, Joshua M Biro,
 683 Anthony D Sorrentino, Jessica L Handley, Sarah Hantzmon, Sophia Bessias, et al. An evaluation
 684 framework for ambient digital scribing tools in clinical applications. *npj Digital Medicine*, 8(1):
 358, 2025.

685

686 Zhenqin Wu, Bharath Ramsundar, Evan N Feinberg, Joseph Gomes, Caleb Geniesse, Aneesh S
 687 Pappu, Karl Leswing, and Vijay Pande. Moleculenet: a benchmark for molecular machine learning.
 688 *Chemical Science*, 9(2):513–530, 2018.

689

690 Qiujie Xie, Qingqiu Li, Zhuohao Yu, Yuejie Zhang, Yue Zhang, and Linyi Yang. An empirical
 691 analysis of uncertainty in large language model evaluations. In *The Thirteenth International
 692 Conference on Learning Representations*, 2025a. URL <https://openreview.net/forum?id=J4xLuCt2kg>.

693

694 Tian Xie and Jeffrey C. Grossman. Crystal graph convolutional neural networks for an accurate
 695 and interpretable prediction of material properties. *Phys. Rev. Lett.*, 120:145301, Apr 2018.
 doi: 10.1103/PhysRevLett.120.145301. URL <https://link.aps.org/doi/10.1103/PhysRevLett.120.145301>.

696

697 Tong Xie, Yuwei Wan, Wei Huang, Zhenyu Yin, Yixuan Liu, Shaozhou Wang, Qingyuan Linghu,
 698 Chunyu Kit, Clara Grazian, Wenjie Zhang, et al. Darwin series: Domain specific large language
 699 models for natural science. *ArXiv preprint ArXiv:2308.13565*, 2023.

700

701 Tong Xie, Yuwei Wan, Yixuan Liu, Yuchen Zeng, Shaozhou Wang, Wenjie Zhang, Clara Grazian,
 702 Chunyu Kit, Wanli Ouyang, Dongzhan Zhou, and Bram Hoex. Darwin 1.5: Large language models
 703 as materials science adapted learners. *ArXiv preprint ArXiv:2412.11970*, 2025b.

702 Yongjun Xu, Xin Liu, Xin Cao, Changping Huang, Enke Liu, Sen Qian, Xingchen Liu, Yanjun Wu,
 703 Fengliang Dong, Cheng-Wei Qiu, et al. Artificial intelligence: A powerful paradigm for scientific
 704 research. *The Innovation*, 2(4), 2021.

705

706 Dan Zhang, Sining Zhoubian, Min Cai, Fengzu Li, Lekang Yang, Wei Wang, Tianjiao Dong, Ziniu
 707 Hu, Jie Tang, and Yisong Yue. Datascibench: An llm agent benchmark for data science. *ArXiv*
 708 preprint *ArXiv:2502.13897*, 2025.

709

710 Di Zhang, Wei Liu, Qian Tan, Jingdan Chen, Hang Yan, Yuliang Yan, Jiatong Li, Weiran Huang,
 711 Xiangyu Yue, Wanli Ouyang, et al. Chemllm: A chemical large language model. *ArXiv preprint*
 712 *ArXiv:2402.06852*, 2024a.

713

714 Kai Zhang, Rong Zhou, Eashan Adhikarla, Zhiling Yan, Yixin Liu, Jun Yu, Zhengliang Liu, Xun
 715 Chen, Brian D Davison, Hui Ren, et al. A generalist vision–language foundation model for diverse
 biomedical tasks. *Nature Medicine*, pp. 1–13, 2024b.

716

717 Tingmei Zhao, Yulong Cai, Yujie Jiang, Xuemei He, Yuquan Wei, Yifan Yu, and Xiaohe Tian. Vaccine
 adjuvants: mechanisms and platforms. *Signal Transduction and Targeted Therapy*, 8(1):283, 2023.

718

719 Lianmin Zheng, Wei-Lin Chiang, Ying Sheng, Siyuan Zhuang, Zhanghao Wu, Yonghao Zhuang,
 720 Zi Lin, Zhuohan Li, Dacheng Li, Eric Xing, et al. Judging llm-as-a-judge with mt-bench and
 721 chatbot arena. *Advances in neural information processing systems*, 36:46595–46623, 2023.

722

723 Jinguo Zhu, Weiyun Wang, Zhe Chen, Zhaoyang Liu, Shenglong Ye, Lixin Gu, Yuchen Duan, Hao
 724 Tian, Weijie Su, Jie Shao, et al. Internvl3: Exploring advanced training and test-time recipes for
 725 open-source multimodal models. *ArXiv preprint ArXiv:2504.10479*, 2025.

726

727

728

729

730

731

732

733

734

735

736

737

738

739

740

741

742

743

744

745

746

747

748

749

750

751

752

753

754

755

756 APPENDIX OVERVIEW
757758 This appendix provides supplementary material to support reproducibility and clarity. It is organized
759 as follows:
760

- 761 • **Appendix A: Dataset Construction**
 - 762 – Additional statistics, distributions, and category breakdown.
- 763 • **Appendix B: Data Preprocessing and Expert Annotation**
 - 764 – B.1 Details of the preprocessing pipeline.
 - 765 – B.2 Details of expert annotation workflow, quality control procedures, and inter-
766 annotator agreement notes.
- 767 • **Appendix C: Representative Q&A Examples**
 - 768 – Selected samples from the benchmark illustrating different knowledge categories.
- 769 • **Appendix D: Formal Framework**
 - 770 – D1. Definitions of formal variables.
 - 771 – D2. Definitions of formal functions.
 - 772 – D3. Definitions of functional transfer relationship.
- 773 • **Appendix E: Evaluation Metrics**
 - 774 – E.1 Mathematical formulations of Semantic Textual Similarity (STS).
 - 775 – E.2 Mathematical formulations of BERTScore.
 - 776 – E.3 Definition of LLM Score and consistency verification between the human expert
777 score.
 - 778 – E.4 Mathematical formulations of Hallucination Rejection Ratio (HRR).
- 779 • **Appendix F: Experimental Analyses**
 - 780 – F.1 Extended results on prompt-following.
 - 781 – F.2 The State-of-the-art model category comparisons.
 - 782 – F.3 Evaluation in visual-related subsets.
 - 783 – F.4 Error visualization analysis of domain-specific models.
- 784 • **Appendix G: Prompts**
 - 785 – G.1 Data generation prompt templates.
 - 786 – G.2 Evaluation prompt templates.
- 787 • **Appendix H: Word Cloud Visualization**
 - 788 – Supplementary visualizations of key concepts and terminology distribution.
- 789 • **Appendix I: Usage of Large Language Models.**
 - 790 – The usage of Large Language Models in this paper.

791 A DETAILED DATA FOR CHART
792793 A.1 DISTRIBUTION OF THE ADJUVANT BENCHMARK
794801 Table 7: Distribution of the Data Types
802

803 Category	804 Open-ended Q&A	805 Hallucination	806 Adjuvants Formal
807 Count	1294	69	1364

807 A.2 DISTRIBUTION OF MLLMs FOR GENERATING Q&A DATA
808

809 A.3 SUBJECTIVE EVALUATION OF MLLMs IN GENERATION

Table 8: Distribution of MLLMs for Generating Q&A Data

Model	DeepSeek-R1	GPT-4o	Claude3.5-Sonnet	Ernie4.0-Turbo
Count	559	471	143	121

Table 9: Subjective Evaluation of MLLMs in Generation

Ability	GPT-4o	Claude3.5	Ernie4.0	DeepSeek-R1
Questioning	8.0	6.4	6.9	7.9
Answering	7.0	6.5	7.4	8.1
Reasoning	7.7	7.1	7.7	8.0
Knowledge Reserve	7.0	6.9	7.1	7.5
Chart Analysis	6.2	5.3	5.0	7.7
Context Utilization	7.2	7.1	6.1	7.8
Instruction Following	8.0	6.5	6.0	7.5

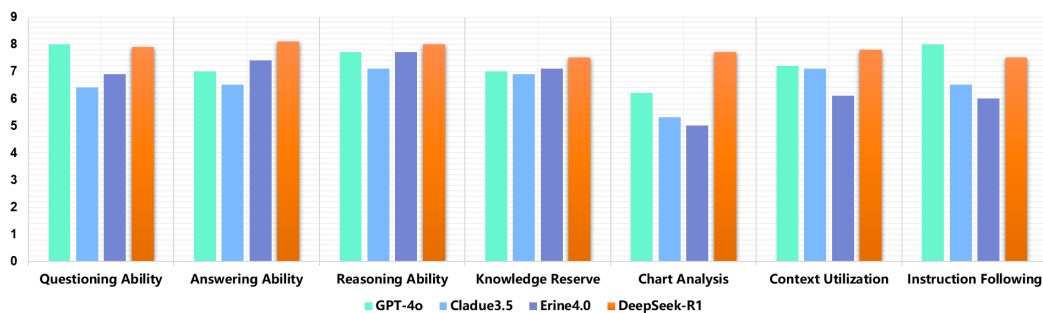
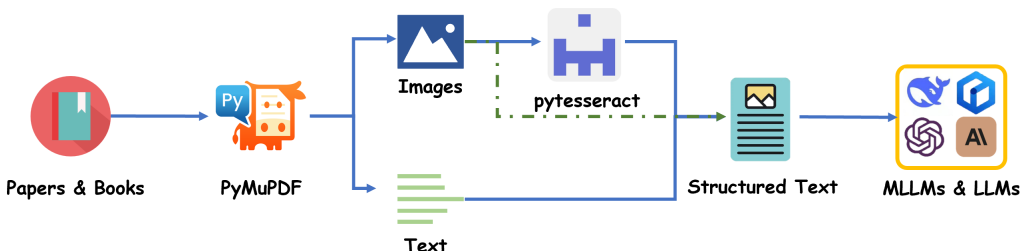


Figure 5: Visualization of Subjective Evaluation in MLLMs Generation

864 **B DATA PREPROCESSING AND EXPERT ANNOTATION DETAILS**
865866 **B.1 DATA PREPROCESSING**
867

868 The raw corpus consisted of 739 peer-reviewed research articles and two classic textbooks in im-
869 munology and vaccine adjuvants. We employed a document parsing pipeline based on PyMuPDF
870 + pytesseract to extract structured text while preserving paragraph hierarchy and separating
871 embedded figures. Both extracted text and figures were then provided as context to multimodal
872 models (e.g., GPT-4o). For unimodal models such as DeepSeek-R1, figures were processed with
873 an OCR engine to obtain textual content, ensuring consistency across evaluations (Fig. 6). All
874 outputs were subsequently reviewed, and only accurate and relevant Q&A pairs were retained in the
875 benchmark.
876

885 **Figure 6: Data preprocessing pipeline.**
886

887 From the processed corpus, 1,500 candidate Q&A items were randomly sampled for expert review.
888

889 **B.2 EXPERT ANNOTATION**
890891 **B.2.1 EXPERT TEAM**
892

893 Annotation was carried out by 13 specialists spanning complementary areas of vaccine research:
894

- 895 • **Infectious disease vaccines:** 1 senior researcher, 2 PhD students, 3 MSc students.
- 896 • **Cancer vaccines:** 1 researcher, 2 PhD students, 2 MSc students.
- 897 • **Bacterial vaccines:** 2 MSc students.

898 All annotators had domain training in immunology or vaccine-related research.
899

900 **B.2.2 EXPERT ANNOTATION WORKFLOW**
901

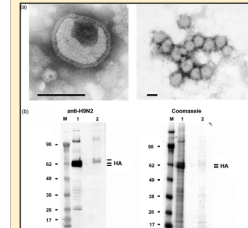
902 Annotation followed standardized guidelines co-developed by AI and immunology experts. The
903 workflow was:

- 904 1. Define goals: establish the first domain-specific benchmark for adjuvant research.
- 905 2. Curate source material: collect high-quality PDFs of papers and textbooks.
- 906 3. Determine data requirements: textbooks for foundational knowledge; research articles for
907 advanced content (mechanisms, design principles, safety).
- 908 4. Pilot phase: generate trial items with MLLMs; refine through expert feedback.
- 909 5. Batch generation: perform large-scale API-based generation once validated.
- 910 6. Annotation protocol: assess each item for (i) correctness of the question, (ii) correctness
911 of the answer, (iii) validity of reasoning, (iv) overall quality. → Incorrect questions ⇒
912 *question hallucinations*; incorrect answers ⇒ *answer hallucinations*.
- 913 7. Standardization: annotators trained to rely exclusively on the source text, avoiding subjective
914 inference.
- 915 8. Validation: first-round expert review followed by quality control from AI researchers before
916 later batches.

918 B.2.3 CONSISTENCY ASSURANCE
919920 To guarantee reliability and minimize subjectivity, we adopted the following measures:
921922

- **Reference standard:** The original source text was defined as the sole criterion for correctness, preventing reliance on prior knowledge or subjective inference.
- **Unified training:** All annotators underwent standardized training and participated in a trial phase before formal labeling.
- **Joint calibration:** Approximately 30% of the samples were jointly annotated to align interpretations across experts.
- **Independent labeling with discussion:** The remaining 70% of samples were labeled independently, with ongoing discussions to resolve uncertainties.

923924 This multi-step protocol ensured consistent, transparent, and reproducible labeling across the benchmark.
925926
927
928
929
930
931
932
933
934
935
936
937
938
939
940
941
942
943
944
945
946
947
948
949
950
951
952
953
954
955
956
957
958
959
960
961
962
963
964
965
966
967
968
969
970
971

972 C CASES FROM ADJUVANT BENCHMARK
973974
975 **Question:** What mechanisms contribute to the diversity of the antigen receptor repertoire in
976 lymphocytes?
977977 **Reasoning Process:** The diversity of antigen receptors is generated through somatic
978 recombination, which includes rearrangements of gene segments and the addition of
979 nucleotides.
980980 **Answer:** Somatic recombination, combinatorial diversity, junctional diversity, and somatic
981 hypermutation contribute to the diversity of antigen receptors.
982983 Figure 7: A Case from Basic Knowledge Open-ended Q&A
984985 **Question:** How does the incorporation of MPLA and α GC into the lipid bilayer affect the
986 kinetics and efficacy of the immune response?
987987 **Reasoning Process:** MPLA and α GC are lipophilic adjuvants incorporated into the lipid bilayer
988 of the particles. MPLA serves as a TLR4 agonist, promoting sustained immune responses
989 through activation of dendritic cells and B cells. α GC, a glycolipid, stimulates invariant
990 natural killer T cells through CD1d presentation, leading to rapid antibody production.
991 These adjuvants enhance both the magnitude and duration of the antibody response by engaging
992 different immune pathways.
993993 **Answer:** MPLA enhances sustained immune responses by activating TLR4 pathways, while α GC
994 promotes rapid antibody production through invariant NKT cell activation. Their
995 incorporation into the lipid bilayer results in a more effective and durable immune response
996 by engaging complementary immune pathways.
997998 Figure 8: A Case from Advanced Knowledge (Biological Principles) Open-ended Q&A
9991000 **Question:** What structural features of the VLPs are revealed by electron microscopy, and why
1001 are these important in Fig?
10021004 **Reasoning Process:** Electron microscopy images show the size and surface features of VLPs,
1005 such as spikes that mimic natural influenza virions, indicating proper assembly and
1006 potential for effective antigen presentation.
10071008 **Answer:** Electron microscopy reveals VLPs with a diameter of 80–120 nm and surface spikes,
1009 indicative of proper assembly and potential to mimic natural virions for effective antigen
1010 presentation.
10111012 Figure 9: A Case from Advanced Knowledge Vision-related Open-ended Q&A
1013

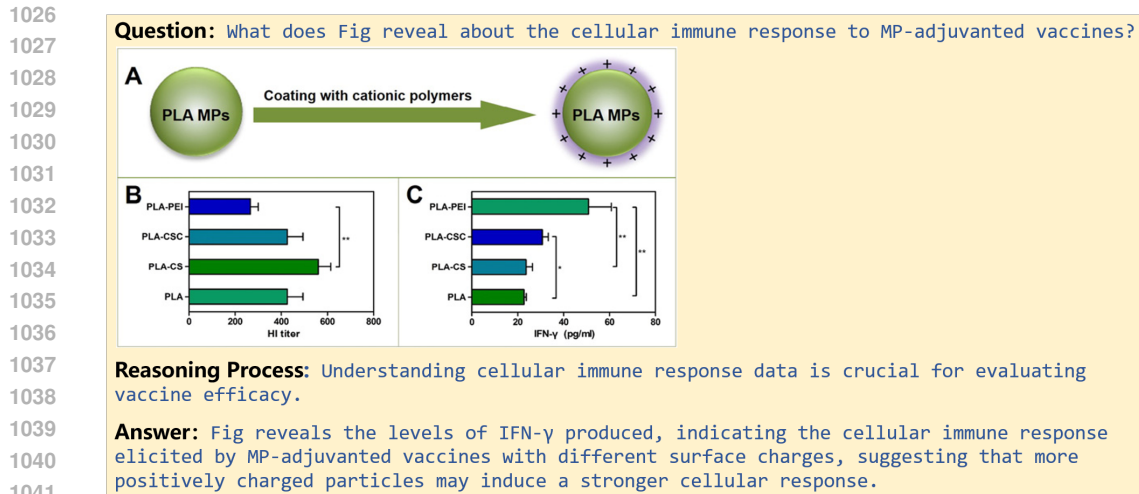


Figure 10: A Case from Advanced Knowledge Vision-related Open-ended Q&A

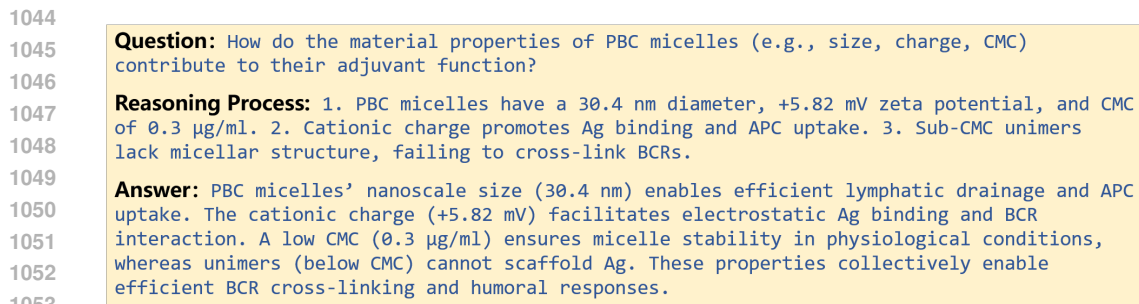


Figure 11: A Case from Advanced Knowledge (Adjuvant Design) Open-ended Q&A

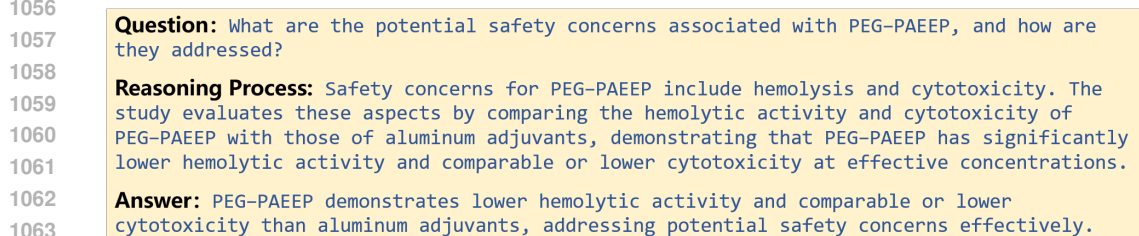


Figure 12: A Case from Advanced Knowledge (Adjuvant Safety) Open-ended Q&A

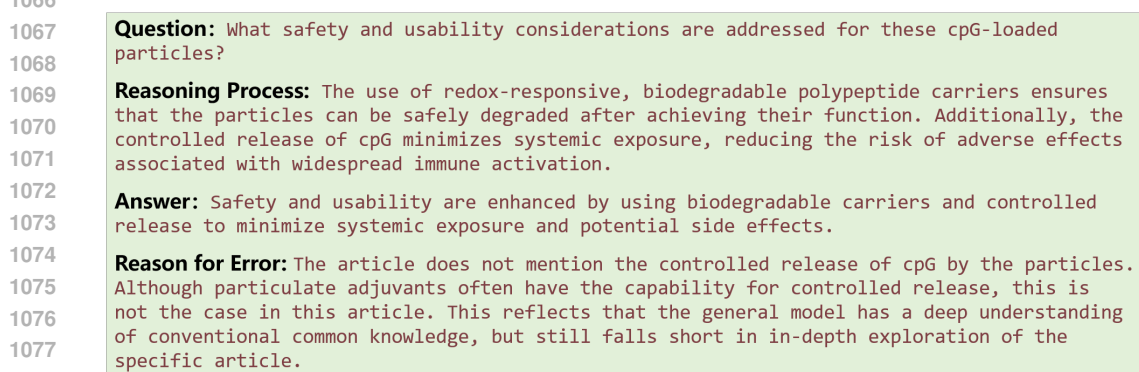


Figure 13: A Case from Question Hallucination Generation by GPT-4o

1080
 1081
 1082
 1083 **Question:** How did the experimental design ensure that the observed immune responses were due
 1084 to the multimerization of antigens on nanoparticles?
 1085 **Reasoning Process:** The design involved comparing immune responses from mice immunized with
 1086 soluble antigens, homotypic nanoparticles, and mosaic nanoparticles. The inclusion of
 1087 different control groups allowed the researchers to isolate the effects of antigen
 1088 multimerization on immune response.
 1089 **Answer:** The experimental design included controls such as soluble antigen immunization,
 1090 which did not elicit cross-reactive responses, thereby demonstrating that multimerization on
 1091 nanoparticles was responsible for the enhanced immunogenicity observed.
 1092 **Reason for Error:** The immune response of soluble antigens and nanoparticle antigens needs to
 1093 be evaluated by the antibody titer (this is the most important) and cross-reaction.

Figure 14: A Case from Answer Hallucination Generation by GPT-4o

1094
 1095
 1096
 1097
 1098
 1099
 1100
 1101 **Question:** How does the design of CpG-loaded particles enhance T cell responses and
 1102 persistent antibodies?
 1103 **Reasoning Process:** The particles are designed to facilitate efficient delivery and prolonged
 1104 release of CpG to pDCs, which are crucial for initiating strong adaptive immune responses.
 1105 By activating pDCs, the particles enhance antigen presentation and costimulatory signals,
 1106 promoting robust T cell activation and aiding the development of long-lasting antibody
 1107 responses.
 1108 **Answer:** Design enhances T cell responses and antibodies by ensuring effective CpG delivery
 1109 and sustained pDC activation, promoting strong adaptive immunity.
 1110 **Reason for Error:** First, the article does not include indicators related to T cells and
 1111 antibodies, so the question itself goes beyond the scope of the article. While the
 1112 reasoning might be correct in general, there is not much content in this article to support
 1113 it, as it only covers enhanced delivery and pDC activation. The answer is even more
 1114 erroneous, as it mistranslates T cells and antibodies and reverses their order with pDC
 1115 activation, while also focusing entirely on aspects that were not mentioned in the article.

Figure 15: A Case from Q&A Hallucination Generation by GPT-4o

1116
 1117
 1118
 1119
 1120
 1121
 1122 **Question:** What further research would be needed to develop these RV-VLPs into a viable
 1123 rabies vaccine candidate?
 1124 **Reasoning Process:** While the article demonstrates promising initial results, several
 1125 additional steps would be needed to develop this into a viable vaccine candidate. These
 1126 would likely include optimizing production and purification processes, conducting more
 1127 extensive immunogenicity studies, evaluating protective efficacy against rabies virus
 1128 challenge, assessing long-term immunity, and conducting safety studies.
 1129 **Answer:** Further research needed would likely include: 1. optimizing RV-VLP production and
 1130 purification processes.

Figure 16: A Case from the Invalid Data Generation by Claude3.5: Incomplete Answer

1134 **D ADJUVANT FORMAL DATA**
11351136 **D.1 DEFINITION OF ADJUVANT FORMAL VARIABLES AND FUNCTIONS**
11371138 **D.1.1 FORMAL VARIABLES**
11391140 **Vaccines (V):** The vaccine, if there are multiple new vaccines, they can be defined as $V = \{Vac_1, Vac_2, \dots, Vac_n\}$.
11411142 **Experimental Group (EG):** Defined as $Vac_e = EG$.
11431144 **Control Group (CG):** Defined as $Vac_e = CG$.
11451146 **Original Viral Surface Antigen (Ag):** The original viral surface antigen defined as Ag . If there are multiple antigens, they can be enumerated as Ag_1, Ag_2, \dots
11471148 **Structural Configurations (Struc):** If antigens possess specific structural configurations, such as particles or dimers, these structures are described and defined as $Struc$. Multiple structures may be defined as $Struc_1, Struc_2, \dots$
11491150 **Antigens in New Vaccines (Ag):** In new vaccines, the antigens employed are similarly defined as Ag .
11511152 **Adjuvant Forms (Struc):** The forms of adjuvants include small molecules, particles, gels, inorganic salts, vesicles, and others. If the literature explicitly specifies the structural forms of adjuvants (e.g., nanoparticles, microparticles, etc.), these adjuvants should be formally incorporated and defined as Adj_1, Adj_2 , and so forth.
11531154 **Movement Variables Related to Vaccine Delivery:** Examples include residence (*Stay at*), drainage (*Drain to*), and targeting (*Target to*), as illustrated below:
11551156 *Stay at the injection site / lung / gut / ... :*
11571158 Stay at $Injection_{site}/Lung/Gut/\dots$
11591160 *Drain to lymph nodes / spleen / bone marrow / ... :*
11611162 Drain to $Lymph_{node}/Spleen/Bone_{marrow}/\dots$
11631164 *Targeted delivery to lymph nodes / spleen / bone marrow / dendritic cells / T cells :*
11651166 Target to $Lymph_{node}/Spleen/Bone_{marrow}/DCs/T_{cells}/\dots$
11671168 **Definitions of Innate Immune Cells:**
11691170 *Conventional Dendritic Cells 1 (cDC1):* $Cell_1 = cDC1$ in injection site
11711172 *Monocyte-derived Macrophages (MoM):* $Cell_2 = MoM$ in peripheral blood
11731174 *Tissue-resident Macrophages (TRM):* $Cell_3 = TRM$ in spleen
11751176 *Neutrophils:* $Cell_4 = Neutrophils$ in lymph nodes
11771178 *Plasmacytoid Dendritic Cells (pDC):* $Cell_5 = pDC$ in peripheral blood
11791180 *Maturation-induced Macrophages:* $Cell_6 = Mature Macrophages$ in tissues
11811182 **Actions of Innate Immune Cells:**
11831184 *Recruitment and Activation of DC:* Recruit / Activate of DC
11851186 *Uptake of Antigen / Adjuvant / Other by DC:* Antigen / Adjuvant / ... Uptake of DC
11871188 *Secretion of Cytokine / Chemokine / Other by DC:* Cytokine / Chemokine / ... Secret of DC
11891190 *Antigen Presentation by DC:* Antigen presentation of DC
11911192 *Migration of DC:* Migrate of DC
11931194 *Phagocytosis by DC:* Phagocytosis of DC
1195

1242 *Secrete*: - Movement refers to the increase in antibody titers, which can be interpreted as an increase
 1243 in antibody secretion.

$$1244 \quad \text{Movement} = \text{Secrete of Ab}$$

1245 *Affinity*: - Movement refers to the enhanced binding of antibodies to viruses, interpreted as an increase
 1246 in affinity.

$$1247 \quad \text{Movement} = \text{Affinity of Ab}$$

1248 *Cross-reactivity*: - Movement refers to the enhanced binding of antibodies to antigens from other
 1249 variants, interpreted as an increase in cross-reactivity.

$$1250 \quad \text{Movement} = \text{Cross-reactivity of Ab}$$

1251 *Neutralization*: - Movement refers to the ability of antibodies to block pathogenic activity through
 1252 target engagement.

$$1253 \quad \text{Movement} = \text{Neutralization by Ab}$$

1254 **Definitions of Other Immune Reactions:**

1255 In the text, there may be some summary-type descriptions of immune responses, such as GC responses
 1256 and T cell responses. Sometimes, it is not appropriate to define them as the above movement variable,
 1257 instead, these immune responses can be directly defined as movement variables.

1258 **Example:** The GC response in the lymph node:

$$1259 \quad \text{Movement} = \text{GC responses in lymph node}$$

1260 D.1.2 FORMAL FUNCTION

1261 **Representation of Composition (Form):** If an antigen Ag_1 forms a structure $Struc_1$, it can be
 1262 expressed as:

$$1263 \quad Form(Struc_1, Ag_1)$$

1264 The function $Form(A, B/C/D/\dots)$ represents the composition and refers to the assembly of
 1265 substances or antigens $B/C/D/\dots$ into A (adjuvants, structures, etc.).

1266 **Loading:** The function $Load(A, B, \text{Inside/Surface}/\dots)$ refers to loading A into the inside or on the
 1267 surface of B .

$$1268 \quad Load(A, B, \text{Inside}) \quad \text{or} \quad Load(A, B, \text{Surface})$$

1269 **Mixing:** The function $Mix(A, B)$ refers to simply blending A and B together.

$$1270 \quad Mix(A, B)$$

1271 **Chemical Coupling:** The function $Link(A, B)$ refers to chemically connecting A to B via chemical
 1272 bonds, protein linkage systems, or linkers.

$$1273 \quad Link(A, B)$$

1274 **Custom Combination Method:** If new combination methods are specified in the literature, they
 1275 should be defined appropriately, for example, a function $Combine(A, B)$ may represent a new
 1276 method of combination.

$$1277 \quad Combine(A, B)$$

1278 D.1.3 FUNCTIONAL TRANSFER RELATIONSHIP

1279 **Comparative Relationships Between Experimental Group and Control Group:**

1280 **Example 1:** Experimental group EG enhances the action (Movement variable) compared to the
 1281 control group CG.

$$1282 \quad EG \text{ Enhance to CG at } \dots/\dots$$

1283 **Example 2:** Experimental group EG reduces the action (Movement variable) compared to the control
 1284 group CG.

$$1285 \quad EG \text{ Reduce to CG at } \dots/\dots$$

1296 **Persistent Comparison:** For continuous comparative relationships, only when the original text
 1297 explicitly contains words such as *prolong*, *extend*, *persistent*, *sustained*, or *durable*, can the persistent
 1298 comparative relationship be established.

1299 **Example 3:** Experimental group EG prolongs the action (Movement variable) compared to the
 1300 control group CG.

1301 EG Prolong to CG at .../...

1302 **Transfer Relationships:**

1303 *Causal relationship:* For causal relationships that are explicitly stated or indicated in the article, use
 1304 the symbol \gg to represent them.

1305 *Comparative relationships and the conjunction:* Use the symbol $\&$ to represent comparative relationships and the conjunction of immune pathways.

1306 *Further extend causal relationships:* After establishing a clear causal inference, it is possible to further extend this causal chain based on existing background knowledge. However, only the actions and indicators explicitly stated in the article may be used, and no new actions can be introduced. Only the existing causal relationships between actions may be supplemented, represented by the symbol \dashrightarrow .

1314 **D.2 THE CASES OF ADJUVANT FORMAL DATA**

1315 **Adjuvant Formal Language:**

```
1316 Ag_1 = Trp2 peptide from melanoma
1317 Adj_1 = PSA micelle
1318 Struc_1 = Cationic micelle
1319 Ag_2 = Form(Struc_1, Ag_1)
1320 Adj_1 = Form(Struc_1, polyethylenimine (PEI-2k)/stearic acid)
1321 Vac1 = Load(Ag_2, Adj_1, Inside) = EG
1322 Vac2 = Mix(Ag_1, Adj_1) = CG1
1323 Vac3 = Ag_1 = CG2
```

1324 **Natural language Text:** The study introduces a novel vaccine formulation where PSA micelles are utilized to deliver the Trp2 melanoma antigen peptide. These micelles demonstrate an average size of 28.7 ± 8.2 nm with a near-perfect encapsulation efficiency of the antigen. The PSA micelles are prepared by conjugating branched PEI-2k with stearic acid, forming an amphiphilic structure. The PSA micelles enhance antigen-specific CTL responses and show a preferential accumulation in draining lymph nodes, thereby minimizing systemic toxicity. This vaccine is compared against controls such as free Trp2 and a mixture of Trp2 with empty PSA micelles to assess its efficacy in enhancing immune responses and inhibiting tumor growth in a murine melanoma model.

1333 Figure 17: A Case from Adjuvant Formal about Adjuvant Design

1350
 1351
 1352
 1353
 1354
 1355
 1356
 1357
 1358
 1359
 1360
 1361
 1362
 1363
 1364
 1365
 1366
 1367

Adjuvant Formal Language:

Adjuvant Definition: Adj = PEG-PAEEP = EG

Control Group Definition: CG = Aluminum adjuvants

Immune Component Definitions:

Movement_1 = HBsAg-specific IgG titers

Cell_1 = IgG-producing B cells in bone marrow

Movement_2 = Differentiate of Cell_1

Combining Comparison Relationships and Immune Components:

EG Enhance to CG at Movement_1

EG Enhance to CG at Movement_2

Causal Relationship Inference:

EG Enhance to CG at Movement_1 >> EG Enhance to CG at Movement_2

Comparative Relationships Extraction to Simplify Causal Chains:

EG to CG

Enhance(Movement_1) >> Enhance(Movement_2)

Natural language Text: The PEG-PAEEP copolymer enhances the immune responses of the HBsAg-VLP vaccine compared to aluminum adjuvants, inducing significantly higher HBsAg-specific IgG titers in mice after the second immunization.

1385
 1386
 1387
 1388
 1389
 1390
 1391
 1392
 1393
 1394
 1395
 1396
 1397
 1398
 1399
 1400
 1401
 1402
 1403

Figure 18: A Case from Adjuvant Formal about Adjuvant Activation and Immune Process

1404
1405 E EVALUATION METRICS

1406 Traditional n-gram-based metrics, which rely on character or token overlap, are not well suited to
 1407 open-ended question answering. They emphasize surface similarity and often miss deeper semantic
 1408 alignment. We therefore adopt **Semantic Textual Similarity (STS)** and **BERTScore**, which operate
 1409 at the semantic level rather than raw overlap. In addition, we report an **LLM-based score** that
 1410 complements embedding metrics by explicitly rating answers along predefined rubrics (similarity,
 1411 rationality, inclusiveness). Together, these metrics provide complementary perspectives and allow for
 1412 more reproducible and transparent evaluation.

1413 To assess hallucination rejection, we leverage hallucination data from the adjuvant benchmark.
 1414 Models are prompted with expert-annotated incorrect Q&A and asked to judge whether a sample
 1415 is invalid; the resulting *hallucination rejection ratio* (HRR) measures the proportion of correctly
 1416 rejected items.

1417
1418 E.1 SEMANTIC TEXTUAL SIMILARITY (STS)

1419
1420 STS evaluates the semantic proximity between two texts via cosine similarity of sentence embeddings.
 1421 We compute embeddings with the **SentenceTransformer** Python module (model:
 1422 **all-mpnet-base-v2**) Reimers & Gurevych (2019).

1423 Given texts T_1 and T_2 with embeddings $\mathbf{E}(T_1)$ and $\mathbf{E}(T_2)$, the score is

$$1424 \quad \text{STS}(T_1, T_2) = \frac{\mathbf{E}(T_1) \cdot \mathbf{E}(T_2)}{\|\mathbf{E}(T_1)\| \|\mathbf{E}(T_2)\|}. \quad (1)$$

1425 The value ranges from -1 to 1 , with larger values indicating stronger semantic alignment.

1426
1427 E.2 BERTSCORE

1428
1429 BERTScore computes token-level semantic similarity using contextual embeddings. For a generated
 1430 text G and a reference C , we form a similarity matrix

$$1431 \quad S_{i,j} = \frac{\mathbf{E}(G_i) \cdot \mathbf{E}(C_j)}{\|\mathbf{E}(G_i)\| \|\mathbf{E}(C_j)\|}, \quad (2)$$

1432 take $P(i) = \max_j S_{i,j}$ as the best match for token G_i , and average:

$$1433 \quad \text{BERTScore} = \frac{1}{|G|} \sum_{i=1}^{|G|} P(i). \quad (3)$$

1434 Scores are normalized to $[0, 1]$ (higher is better). Compared with STS (sentence-level semantics),
 1435 BERTScore emphasizes token-level precision. For our **BERTScore calculations, we use the**
 1436 **scibert_scivocab_uncased** model Beltagy et al. (2019) **with its corresponding tokenizer**.

1437
1438 E.3 LLM SCORE

1439 To complement embedding-based metrics, we employ an **LLM-based evaluation** with GPT-4o and
 1440 DeepSeek-R1. Each candidate answer is assessed along three dimensions:

- 1441 • **Similarity Score (SS):** factual alignment with the expert reference answer.
- 1442 • **Rationality Score (RS):** scientific soundness and logical coherence of the reasoning process.
- 1443 • **Inclusiveness Score (IS):** coverage of essential points and completeness in addressing the
 1444 question.

1445 Each dimension is scored on a $[0, 10]$ scale, with the following interpretation in the context of adjuvant
 1446 knowledge:

- 1447 • **0–3 (poor):** major factual errors or incoherent reasoning, reflecting a lack of basic under-
 1448 standing of adjuvant concepts.

- **4–6 (adequate):** partially correct and logically consistent answers, but with noticeable gaps or oversimplifications in immunological mechanisms or design principles.
- **7–10 (strong):** scientifically consistent, well-reasoned, and comprehensive answers that demonstrate a solid grasp of adjuvant biology and related immunological processes.

These three dimensions are deliberately chosen for the adjuvant domain: factual alignment (SS) captures accuracy of immunological details, rationality (RS) reflects whether the explanation is mechanistically plausible, and inclusiveness (IS) ensures that answers go beyond isolated facts to integrate the multifaceted nature of adjuvant design and immune modulation.

Why LLM Score is valid: Using large language models as evaluators (“LLM-as-a-judge”) has become a widely adopted practice in open-ended evaluation. Prior studies in general NLP benchmarks demonstrate that LLM-based judgements correlate strongly with human preferences when prompts and rubrics are standardized, and also analyze typical biases such as verbosity or self-preference Zheng et al. (2023); Dubois et al. (2024); Kim et al. (2024); Panickssery et al. (2024); Xie et al. (2025a).

Beyond general-purpose tasks, recent work shows that LLM-based evaluation is also effective in scientific and biomedical domains. For instance, scientific question answering and biomedical information extraction have employed rubric-guided LLM judges to approximate expert assessment D’Souza et al. (2025); Laskar et al. (2025). In the medical domain, Wang et al. (2025) integrated LLM evaluators into a formal framework for clinical ambient scribing, published in a Nature journal. Similarly, mathematical reasoning tasks have used LLM judges to assess solution validity under verifiable criteria Stephan et al. (2024). These precedents confirm that LLM-as-a-judge is not only scalable but also increasingly recognized across scientific subfields.

In our setup, we (i) fix prompts and decoding parameters to minimize variance, (ii) average scores from two high-performing evaluators (GPT-4o and DeepSeek-R1) to reduce single-model bias, and (iii) complement LLM-based scores with embedding metrics (STS/BERTScore) for transparency and reproducibility. This multi-perspective design yields a reliable proxy for expert assessment while keeping annotation costs tractable, aligning with best practices reported across both general and scientific domains.

E.3.1 EXPERIMENT OF CONSISTENCY VERIFICATION BETWEEN LLM SCORE AND HUMAN EXPERT SCORE

To verify the effectiveness of using LLMs as judges in the field of adjuvants, we conducted a consistency test between LLM scores and human expert scores. Specifically, we randomly selected 100 responses from all models, with 50 evaluated by GPT-4o and the other 50 evaluated by DeepSeek-R1. These 100 samples were then submitted to human experts for evaluation, using criteria that were completely consistent with those used for the LLM scores. The results are presented in Table 10.

Table 10: Consistency Verification Between LLM Scores and Human Expert Scores

Scoring Model	Rating Dimension	Pearson Correlation	Spearman Correlation	Kendall Correlation
GPT-4o	Similarity	0.8412	0.8469	0.7752
	Rationality	0.8006	0.6342	0.5793
	Inclusiveness	0.8135	0.7487	0.6749
	Avg	0.8407	0.8044	0.7084
DeepSeek-R1	Similarity	0.9145	0.9236	0.8185
	Rationality	0.8767	0.8456	0.7732
	Inclusiveness	0.8636	0.8749	0.7613
	Avg	0.9125	0.9247	0.8019
All	Similarity	0.8854	0.8920	0.8019
	Rationality	0.8443	0.7986	0.7239
	Inclusiveness	0.8461	0.8416	0.7413
	Avg	0.8803	0.8871	0.7739

The experiment and visualization (as shown in Fig 19) demonstrate high reliability in using these models as scorers. Both GPT-4o and DeepSeek show strong linear correlations with expert scores, particularly in the Similarity dimension, where GPT-4o achieves a Pearson correlation of 0.8412 and

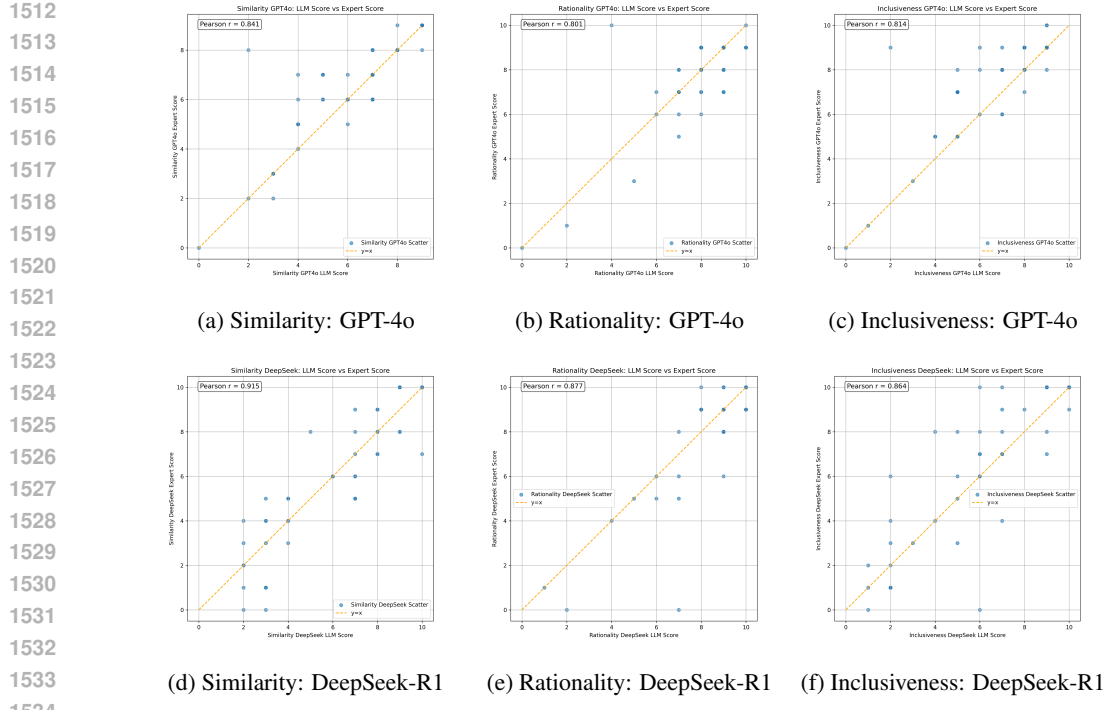


Figure 19: LLM Score vs. Expert Score

DeepSeek reaches 0.9145. Although GPT-4o's correlations are slightly lower, it remains consistently strong across all dimensions, indicating that both models align well with expert evaluations and are effective scoring agents.

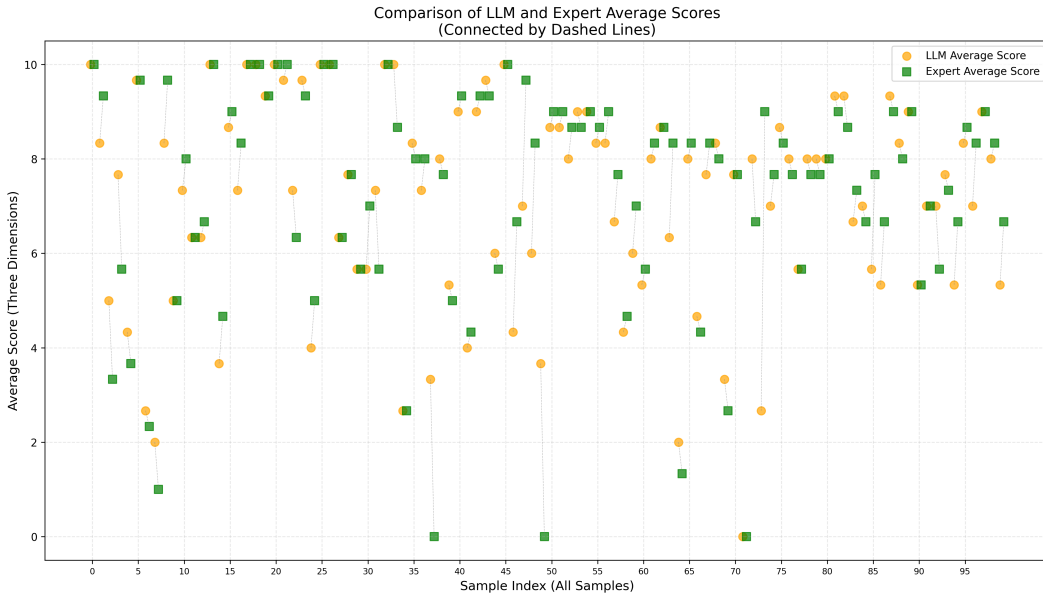


Figure 20: Comparison of LLM and Expert Average Scores

Further analysis using Spearman correlation reveals that DeepSeek outperforms GPT-4o, especially in the Similarity (0.9236) and Rationality (0.8456) dimensions. Despite GPT-4o's lower performance in Rationality (0.6342), it still maintains a reasonable level of ranking consistency, reinforcing its validity as a scorer. The Kendall correlation results mirror these findings, with DeepSeek consistently showing higher scores across all dimensions, particularly in Similarity (0.8185) and Rationality (0.7812).

1566 (0.7732). Although GPT-4o’s performance is lower in comparison, it remains within an acceptable
 1567 range, particularly in Similarity (0.7752), which indicates a strong consistency in ranking with expert
 1568 scores.

1569 Overall, both GPT-4o and DeepSeek show strong alignment with expert scores, as demonstrated in
 1570 Fig 20. The average scores across the three dimensions for both the LLM and expert evaluations
 1571 largely overlap, confirming their reliability as scorers for this task. While DeepSeek slightly outper-
 1572 forms GPT-4o, particularly in Pearson and Spearman correlations, both models exhibit substantial
 1573 effectiveness and are well-suited for scoring tasks in this domain.

1577 E.3.2 THE PROMPT OF LLM SCORE

1579 The Prompt of LLM Score Evaluation

1581 You are an expert in immunology and adjuvant design, with great achievements in immunol-
 1582 ogy and adjuvant design. With the aim of simplifying the thinking process, please score the
 1583 model’s answers and labels (out of 10 points) based on the similarity between the answers and
 1584 labels, the reasonableness of the answers, and whether the answers incorporate the meaning
 1585 of the labels. Finally, please provide the results in the following format:

1586 **Similarity Score:** x

1587 **Rationality Score:** x

1588 **Inclusiveness Score:** x

1592 E.4 HALLUCINATION REJECTION RATIO (HRR)

1594 The hallucination rejection ratio (HRR) quantifies a model’s ability to detect and resist hallucinated
 1595 content:

$$1598 \text{HRR} = \frac{\text{Number of correctly rejected hallucinated samples}}{\text{Total hallucinated samples}} \times 100\%.$$

1602 Here, the numerator counts expert-labeled hallucinated Q&A pairs that the model successfully
 1603 flags as invalid. A higher HRR indicates stronger robustness, which is particularly important in
 1604 safety-sensitive biomedical applications.

1606 **Prompt design.** The evaluation prompt explicitly defines the label mapping: “*Yes*” means the Q&A
 1607 is scientifically valid, while “*No*” means it contains hallucination (i.e., invalid claims). Additional
 1608 criteria are listed (factual errors, logical inconsistencies, causal reversal, pseudo-scientific claims,
 1609 domain irrelevance, or incomplete answers). In practice, the model is instructed to return “*No*”
 1610 whenever any of these problems occur, and “*Yes*” only when the Q&A is entirely correct and domain-
 1611 relevant. The requirement to “strictly return Yes or No” ensures output consistency and facilitates
 1612 automatic scoring; it does not prevent verification, since the ground truth hallucination labels were
 1613 already provided by domain experts during dataset construction.

1614 **Sample size.** The current hallucination dataset consists of 69 high-quality, expert-annotated examples.
 1615 While relatively small, it represents the first curated hallucination resource in the adjuvant domain. To
 1616 mitigate sample-size concerns, we report mean HRR with standard deviations over ten repeated trials.
 1617 This provides an uncertainty estimate and ensures that performance differences reflect systematic
 1618 model behavior rather than random variation.

1619 Together, this setup ensures that HRR measures what it is intended to capture: whether models can
 1620 resist generating or endorsing scientifically invalid claims in immunology and adjuvant science.

1620 E.4.1 THE PROMPT OF HALLUCINATION EVALUATION
16211622 The Prompt of Hallucination Evaluation
16231624 You are an expert in immunology and adjuvant design, with great achievements in the
1625 immunology and adjuvant fields. Determine if the provided **Question** or its corresponding
1626 **Answer** contains scientifically invalid claims in the fields of **Biology**, **Immunology**, or
1627 **Adjuvant Science**. Return **only** "Yes" (**valid**) or "No" (**invalid**) without explanations.
16281629 **Input Format:**
1630 - **Question:** [Insert question text]
1631 - **Answer:** [Insert answer text]
16321633 **Evaluation Criteria**
1634 Return "No" if ANY of the following apply (including but not limited to):
1635 **1.Factual Errors**
1636 - Contradicts established scientific consensus.
1637 **2.Logical Inconsistencies**
1638 - Self-contradictory statements.
1639 **3.Causal Reversal**
1640 - Inverts cause-effect relationships.
1641 **4.Pseudo-Scientific Claims**
1642 - Unproven theories.
1643 **5.Domain Irrelevance**
1644 - Topics outside biology/immunology/adjuvant science.
1645 **6.Incomplete Answers - Missing critical steps/mechanisms.**
16461647 Return "Yes" ONLY if the Q&A pair is scientifically accurate, logically consistent, and
1648 domain-relevant.
16491650 **Response Requirement:**
1651 - Strictly return "Yes" or "No" in a single line.
1652 - No markdown, formatting, or additional text.
1653
1654
1655
1656
1657
1658
1659
1660
1661
1662
1663
1664
1665
1666
1667
1668
1669
1670
1671
1672
1673

1674 F EXPERIMENT ANALYSIS
16751676 F.1 EVALUATION OF PROMPT-FOLLOWING
16771678 We assessed the prompt-following ability of 11 closed-source and 18 open-source MLLMs under
1679 identical hyperparameter settings. Results are summarized in Table 11.1680 **Closed-source vs. open-source.** Closed-source models consistently outperform open-source counter-
1681 parts, showing higher average STS and BERTScore when prompts are introduced. This indicates
1682 stronger instruction parsing and more reliable adherence to task requirements.
16831684 **Performance shifts in open-source models.** Interestingly, while prompts generally improved
1685 semantic alignment (higher STS/BERTScore), several open-source models exhibited a *drop in overall*
1686 *LLM Score*. Manual inspection suggests that prompts sometimes pushed these models toward verbose
1687 or rigidly formatted answers, inflating token-level similarity but reducing factual soundness and
1688 completeness. This mismatch highlights a trade-off between surface-level semantic alignment and
1689 deeper reasoning accuracy in open-source systems.
16901691 **Model-specific variability.** Domain-specific systems such as BioGPT-Large perform particularly
1692 poorly without explicit guiding phrases, in some cases even degrading compared to their no-prompt
1693 baseline. For example, BioGPT-Large often required a deterministic prefix (e.g., "The answer
1694 is:") to produce stable and interpretable outputs. Without such hints, its responses tended to diverge
1695 from the expected format, which explains its negative improvement in Table 11 and 5.
16961697 **inference Model vs. Think Model.** "Think" models with explicit reasoning mechanisms show
1698 relatively stable performance when prompts are added, compared to inference-only models. This
1699 stability likely stems from their multi-step reasoning pathways, which already encourage adherence
1700 to task constraints. By contrast, inference models exhibit more variability, suggesting that they are
1701 more sensitive to prompt phrasing. Notably, gains in STS and BERTScore for both families are partly
1702 explained by prompts eliciting more domain-specific terminology, which boosts surface alignment
1703 metrics.
17041705 **Summary.** These findings highlight prompt-following as a key dimension of model robustness.
1706 However, improvements in surface-level metrics do not always translate to better overall judgment
1707 (LLM Score), particularly for open-source systems. This underscores the need for evaluation
1708 frameworks that disentangle genuine reasoning gains from superficial prompt-induced artifacts.
17091710
1711
1712
1713
1714
1715
1716
1717
1718
1719
1720
1721
1722
1723
1724
1725
1726
1727

1728

1729

1730

1731

1732

1733

1734

1735

1736

1737

1738

1739

1740

1741

1742

Table 11: Evaluation of Adjuvants in Open-ended Q&A (Without prompt)

1743

1744

1745

1746

Model Category	STS Score	BertScore	LLM Score (GPT-4o)			LLM Score (DeepSeek-R1)			LLM Score Avg			
			SS	RS	IS	SS	RS	IS				
Closed-source MLLMs												
<i>Inference Models</i>												
GPT-4o	0.7190	0.5693	6.3	8.2	6.6	6.7	8.5	6.5	7.1			
GPT-4.1	0.7150	0.5219	6.6	8.1	6.9	7.4	8.9	7.4	7.7			
Cladue3.5	0.7153	0.5598	5.8	7.8	6.2	6.4	8.6	6.6	6.9			
Cladue3.7	0.7323	0.5596	6.3	8.0	6.5	6.8	8.6	6.8	7.2			
Gemini1.5-Pro	0.7123	0.5596	6.2	8.1	6.4	6.7	8.6	6.7	7.1			
Gemini2.0-Pro	0.6927	0.5362	6.0	7.9	6.3	6.6	8.5	6.8	7.0			
Gemini2.5-Pro	0.6927	0.5362	6.5	8.2	6.8	7.1	8.7	7.0	7.4			
Ernie3.5	0.7121	0.5502	5.8	7.8	6.2	6.2	8.0	6.0	6.7			
Ernie4.0	0.7337	0.6027	6.1	7.7	6.1	6.1	7.9	5.6	6.6			
Doubaol1.5-Pro	0.7093	0.5490	6.0	7.8	6.2	6.6	8.3	6.6	6.9			
<i>Think Models</i>												
OpenAI-o1	0.7310	0.5818	6.9	8.5	7.1	7.3	8.9	7.3	7.7			
Average	0.7150	0.5569	6.2	8.0	6.5	6.7	8.5	6.7	7.1			
Open-source MLLMs												
<i>Inference Models</i>												
DeepSeek-V3	0.7255	0.5254	6.5	8.2	6.8	7.4	8.8	7.5	7.5			
LLaVA1.5-7B	0.7115	0.5763	5.1	6.5	4.8	5.0	6.2	4.3	5.3			
LLaVA1.5-13B	0.7140	0.5888	5.3	7.0	5.2	5.4	6.8	4.7	5.7			
Qwen2.5-VL-7B	0.7008	0.5513	5.5	7.6	5.8	5.7	7.5	5.4	6.3			
Qwen2.5-VL-72B	0.7054	0.5723	5.7	7.5	5.9	5.9	7.8	5.7	6.4			
Internvl2.5-8B	0.6824	0.5606	5.0	6.7	5.0	5.1	6.4	4.6	5.5			
Internvl2.5-78B	0.7156	0.5675	5.8	7.6	5.9	6.0	7.6	5.7	6.4			
Internvl3.0-8B	0.7111	0.5657	5.4	7.3	5.5	5.5	7.1	5.2	6.0			
Internvl3.0-78B	0.7198	0.5679	6.0	7.8	6.2	6.2	8.0	6.0	6.7			
InstructBlip-13B	0.6017	0.5711	4.8	6.1	4.4	4.9	6.1	4.1	5.1			
Idefics-B	0.6632	0.5002	4.9	6.3	4.6	4.9	5.8	4.2	5.1			
<i>Think Models</i>												
DeepSeek-R1	0.7360	0.5485	6.6	8.4	7.0	7.3	8.8	7.5	7.6			
Qwen3-8B	0.7186	0.5297	6.1	8.1	6.5	6.9	8.6	7.0	7.2			
Qwen3-32B	0.7193	0.5316	6.6	8.1	6.8	7.3	8.8	7.5	7.5			
Qwen3-30B-A3B	0.7174	0.5302	6.3	8.2	6.7	7.1	8.7	7.2	7.4			
Qwen3-235B-A22B	0.7262	0.5443	6.5	8.4	6.9	7.2	8.8	7.4	7.5			
<i>Domain-Specific Models</i>												
Darwin	0.6265	0.6253	4.3	5.4	3.7	3.9	5.2	3.0	4.3			
BioGPT-Large-PubMedQA	0.5995	0.4665	3.1	4.0	2.8	3.2	4.4	2.7	3.4			
Average	0.6942	0.5514	5.5	7.2	5.6	5.8	7.3	5.5	6.2			

1769

1770

1771

1772

1773

1774

1775

1776

1777

1778

1779

1780

1781

1782 F.2 THE STATE-OF-THE-ART MODELS VISUALIZATION ANALYSIS
1783

1784 We randomly selected two Q&A pairs for visualization of GPT-o1 and DeepSeek-R1. The results are
1785 shown in Fig. 21 and Fig. 22.

1786 Fig. 21 illustrates that DeepSeek-R1 tends to emphasize specific molecular-level mechanisms, whereas
1787 GPT-o1 provides higher-level framework descriptions. DeepSeek-R1’s responses align more closely
1788 with the style of professional scientific literature, highlighting systematic mechanisms and technical
1789 details, making it suitable for readers seeking in-depth understanding. In contrast, GPT-o1 produces
1790 more concise and accessible answers, which better serve audiences with less biological background
1791 by facilitating a quick grasp of core logic. These differences likely reflect variations in training data
1792 and design objectives.

1793 By contrast, Fig. 22 demonstrates a case where both models perform poorly. The example concerns
1794 the comparison of polyclonal antibody responses elicited by RBD-NP and HexaPro S vaccines in non-
1795 human primates against SARS-CoV-2 RBD mutations, particularly at site 484. Both models attempt
1796 to analyze differences in antibody responses across vaccine platforms, but their reasoning and depth
1797 vary significantly. GPT-o1’s response remains general and framework-driven, while DeepSeek-R1
1798 integrates more domain-specific knowledge but at the cost of over-speculation.

1799 Both models, however, exhibit a similar misconception: they assume that nanoparticles can evade
1800 the E484K mutation. In reality, relevant studies indicate that both RBD-NP and HexaPro S remain
1801 vulnerable to E484K (as shown in the ground truth answer), underscoring the importance of the
1802 antibody binding site at position 484. Neither model captures this crucial detail, instead incorrectly
1803 assuming that nanoparticle polyvalence confers resistance, while full-length proteins are more affected.
1804 This reflects a naive generalization from antigenic polyvalence to mutation resilience.

1805 This case highlights the limitations of current general-purpose models in handling fine-grained
1806 immunological knowledge. It underscores the need for specialized models fine-tuned with domain-
1807 specific data to achieve reliable reasoning in highly specialized biomedical contexts.

1809 F.3 EVALUATION OF TOP 5 MLLMs IN VISUAL-RELATED SUBSETS
1810

1811 We selected the *Top5* MLLMs that performed the best across the entire Open-ended Q&A when using
1812 the same OCR engine (as shown in Fig 5). These models were then evaluated on a visually-related
1813 subset, utilizing their native multimodal capabilities.

1815 Table 12: Evaluation of Adjuvants in Open-ended Q&A Visual-related Subsets (With prompt)
1816

Model Category	STS Score	BertScore	LLM Score (GPT-4o)			LLM Score (DeepSeek-R1)			LLM Score Avg
			SS	RS	IS	SS	RS	IS	
OCR Engine									
GPT-4o	0.7015	0.5729	6.3	7.9	6.7	5.6	9.1	5.9	7.0
GPT-4.1	0.7053	0.5442	7.2	8.5	7.6	6.9	9.3	7.0	7.8
Cladue3.7	0.7205	0.5720	6.6	8.0	6.9	6.3	9.2	6.7	7.3
Gemini2.5-Pro	0.7111	0.5787	6.5	8.0	6.8	6.5	9.5	6.4	7.3
OpenAI-o1	0.7436	0.6222	7.0	8.3	7.1	6.9	9.5	6.8	7.6
Average	0.7164	0.5780	6.7	8.1	7.0	6.4	9.3	6.6	7.4
Multimodal Capability									
GPT-4o	0.7083	0.5889	6.5	7.9	6.6	6.0	9.0	6.1	7.0
GPT-4.1	0.7019	0.5255	7.0	8.3	7.3	6.9	9.4	7.0	7.7
Cladue3.7	0.6936	0.5675	5.8	7.5	6.3	6.0	9.3	6.3	6.9
Gemini2.5-Pro	0.6913	0.5628	6.0	7.7	6.4	6.1	9.2	6.3	7.0
OpenAI-o1	0.7390	0.6217	7.3	8.5	7.4	7.2	9.4	6.9	7.8
Average	0.7068	0.5733	6.5	8.0	6.8	6.4	9.3	6.5	7.3

1830 The result is shown in Table 12, When comparing the two settings (OCR-based input vs. native
1831 multimodal capability), an intriguing trend emerges: some models actually perform worse when
1832 relying on their native multimodal abilities. Overall, OCR-engine preprocessing provides more stable
1833 results across semantic similarity metrics (STS/BertScore) and LLM-based evaluations (SS, RS, IS).
1834 Although certain models, such as OpenAI-o1, maintain strong performance under the multimodal
1835 setting, several general-purpose MLLMs demonstrate noticeable degradation when tasked with
interpreting biological and adjuvant-related visualizations.

1836
1837

We hypothesize two main reasons for this discrepancy:

1838
1839
1840

1. **Lack of domain-specific expertise:** General-purpose multimodal models excel in everyday visual-language tasks but lack optimization for specialized biomedical charts and adjuvant-related diagrams, leading to misinterpretations.
2. **Task representation gap:** OCR-based pipelines provide structured textual input, reducing ambiguity. In contrast, multimodal settings require models to jointly handle visual parsing and domain reasoning, which increases task complexity and may reduce overall performance.

1841

In summary, this experiment indicates that relying solely on the native multimodal capabilities of current MLLMs may not be the most effective approach for domain-specific research tasks. While multimodal models show promise, traditional OCR-based preprocessing provides a more consistent and reliable input format, particularly when dealing with complex and specialized biomedical content. Future research should focus on improving multimodal reasoning by incorporating specialized visual inputs related to biomedical and adjuvant-specific domains.

1844

Furthermore, in this study, all models were evaluated using a unified OCR engine. This approach was chosen to ensure consistency across evaluations by standardizing the input format, thus minimizing potential biases caused by variations in how models handle visual data. Given the specialized nature of the adjuvant-related visualizations, OCR preprocessing offers a structured and reliable form of textual input, which reduces the risk of misinterpretation by models that may not be fully optimized for this domain.

1856

1857

1858

1859

1860

1861

1862

1863

1864

1865

1866

1867

1868

1869

1870

1871

1872

1873

1874

1875

1876

1877

1878

1879

1880

1881

1882

1883

1884

1885

1886

1887

1888

1889

1890
 1891 **Question:** How do sonicated reduced cancer cells (sRCCs) promote the recruitment and
 1892 activation of antigen-presenting cells (APCs)?
 1893 **Ground Truth Answer:** sRCCs loaded with adjuvants like CpG promote the recruitment and
 1894 activation of APCs by enhancing the uptake kinetics and magnitude of adjuvant uptake,
 1895 leading to increased DC activation and cytokine production.
 1896 **OpenAI-o1 Answer:** Sonicated reduced cancer cells (sRCCs) promote the recruitment and
 1897 activation of antigen-presenting cells (APCs) by exposing tumor-associated antigens and
 1898 releasing immunostimulatory signals often referred to as damage-associated molecular
 1899 patterns (DAMPs). When cancer cells undergo mechanical disruption via sonication, they break
 1900 apart and release intracellular contents, including proteins, DNA, and other molecules
 1901 capable of activating pattern recognition receptors on APCs.
 1902 Key points of this process include:
 1903 - Exposure of tumor antigens: Sonication reveals previously hidden or
 1904 intracellular tumor antigens. These antigens, now accessible in the extracellular
 1905 environment, can be taken up by nearby dendritic cells and macrophages.
 1906 - Liberation of DAMPs: Molecules such as HMGB1, ATP, and heat shock proteins are released upon cell
 1907 membrane disruption. These DAMPs serve as potent danger signals that bind to
 1908 pattern recognition receptors (e.g., Toll-like receptors) on APCs, triggering their
 1909 maturation and promoting proinflammatory cytokine production.
 1910 - Enhanced antigen presentation: Once dendritic cells internalize these tumor-associated antigens, they process
 1911 them and present antigenic peptides on MHC class I and II molecules, effectively priming T
 1912 cells against tumor cells.
 1913 - Local inflammatory milieu: The release of DAMPs and proinflammatory cytokines from activated APCs also helps recruit additional immune cells,
 1914 amplifying the local inflammatory response. This heightened environment fosters an improved
 1915 recruitment of other effector cells, including T cells and natural killer cells,
 1916 facilitating a broader antitumor response.
 1917 Overall, the combination of tumor-specific
 1918 signals (antigens) and danger signals (DAMPs) from sRCCs acts as an immunologic
 1919 alarm, mobilizing and activating professional APCs in the tumor microenvironment,
 1920 thereby contributing to a more robust and targeted antitumor immune response.
 1921
 1922 **LLM Scores:**
 1923 - GPT-4o: Similarity score: 5 Rationality score: 8 Inclusiveness score: 6
 1924 - DeepSeek-R1: Similarity score: 7 Rationality score: 9 Inclusiveness score: 7
 1925
 1926 **DeepSeek-R1 Answer:** Sonicated reduced cancer cells (sRCCs) enhance the recruitment and
 1927 activation of antigen-presenting cells (APCs) through several interconnected
 1928 mechanisms:
 1929 - Release of Damage-Associated Molecular Patterns (DAMPs):
 1930 Sonication disrupts cancer cells, releasing intracellular DAMPs such as ATP, HMGB1, heat
 1931 shock proteins, and nucleic acids. These molecules bind to pattern recognition receptors
 1932 (PRRs; e.g., TLRs, RAGE, NLRP3) on APCs, triggering their activation. For example:
 1933 - ATP activates the P2X7 receptor, promoting NLRP3 inflammasome formation and IL-1 β
 1934 secretion.
 1935 - HMGB1 interacts with TLR4 or RAGE, inducing pro-inflammatory cytokine
 1936 production.
 1937 - Nucleic acids engage endosomal TLRs (e.g., TLR3, TLR7/9) or
 1938 cytosolic sensors (cGAS-STING), driving type I interferon responses.
 1939 - Enhanced Antigen Availability and Uptake:
 1940 Sonic fragmentation increases the surface area and
 1941 accessibility of tumor antigens. Smaller cellular debris facilitates efficient phagocytosis
 1942 by APCs, enabling robust antigen processing and presentation via MHC I/II. This promotes
 1943 cross-presentation to CD8 $^{+}$ T cells, critical for antitumor immunity.
 1944 - Chemokine-Mediated Recruitment:
 1945 DAMP signaling induces stromal or immune cells to secrete
 1946 chemokines (e.g., CCL2, CCL5, CXCL10), recruiting monocytes, dendritic cells, and
 1947 macrophages to the tumor site. HMGB1 and ATP also directly chemoattract APCs.
 1948 - Exposure of "Eat-Me" Signals:
 1949 Sonicated cells may expose phosphatidylserine on
 1950 their surface, a marker recognized by phagocytic receptors (e.g., Tim-4, TAM receptors) on
 1951 APCs, enhancing engulfment of apoptotic bodies.
 1952 - Reduction of Immunosuppressive Factors:
 1953 Sonication inactivates live cancer cells, potentially diminishing secretion
 1954 of immunosuppressive cytokines (e.g., IL-10, TGF- β), thereby relieving APC inhibition and
 1955 fostering a pro-inflammatory milieu.
 1956 - Microparticle/Exosome Formation:
 1957 Ultrasonication may generate microvesicles or exosomes carrying tumor antigens and DAMPs,
 1958 which efficiently deliver activation signals to APCs via membrane fusion or
 1959 endocytosis.
 1960 Summary:
 1961 sRCCs act as an endogenous adjuvant by releasing DAMPs and
 1962 tumor antigens, recruiting APCs via chemokines, and activating them through PRR engagement.
 1963 This primes APCs for antigen presentation and co-stimulatory molecule upregulation (e.g.,
 1964 CD80/86), bridging innate and adaptive antitumor immunity.
 1965
 1966 **LLM Scores:**
 1967 - GPT-4o: Similarity score: 6 Rationality score: 8 Inclusiveness score: 7
 1968 - DeepSeek-R1: Similarity score: 9 Rationality score: 9 Inclusiveness score: 9

Figure 21: The Cases of GPT-4o and DeepSeek-R1

1944
 1945 **Question:** How do the polyclonal antibody responses elicited by RBD-NP in non-human primates
 1946 (NHPs) compare to those from HexaPro S vaccination in terms of resilience to SARS-CoV-2 RBD
 1947 mutations, particularly at position 484?
 1948 **Ground Truth Answer:** Both RBD-NP and HexaPro S elicited polyclonal antibodies with similar
 1949 resilience to most RBD mutations, but mutations at position 484 (e.g., E484K) reduced
 1950 neutralization significantly (9-12-fold). This indicates a shared reliance on antibodies
 1951 targeting the RBM around residue 484, a key epitope for both vaccines.
 1952 **OpenAI-o1 Answer:** Studies comparing these two immunogen formats in NHPs generally find that
 1953 RBD-NP immunization drives a focused yet diversified anti-RBD response that is relatively less
 1954 affected by single RBD mutations (including at E484) compared to antibodies elicited by the
 1955 full-length HexaPro S. Because the RBD is presented at high density on nanoparticles, the
 1956 immune system is tuned toward multiple overlapping neutralizing epitopes on the RBD.
 1957 Consequently, even though E484 is an important escape site, RBD-NP-polyclonal sera tend to
 1958 retain better neutralization of E484-mutant viruses than sera raised against the entire spike
 1959 (HexaPro S), whose overall response can be more impacted by point mutations in critical RBD
 1960 sites.
 1961 **LLM Scores:**
 1962 - GPT-4o: Similarity score: 5 Rationality score: 7 Inclusiveness score: 6
 1963 - DeepSeek-R1: Similarity score: 6 Rationality score: 7 Inclusiveness score: 5
 1964 **DeepSeek-R1 Answer:** The comparison of polyclonal antibody responses elicited by RBD-NP
 1965 (Receptor Binding Domain nanoparticle) and HexaPro S (stabilized full-length spike protein)
 1966 vaccines in non-human primates (NHPs) regarding resilience to SARS-CoV-2 RBD mutations at
 1967 position 484 (e.g., E484K) involves several key considerations:
 1968 - **RBD-NP**: Presents the RBD in a repetitive, multivalent nanoparticle format, which enhances B cell receptor cross-linking and germinal center responses. This promotes a **broad, polyclonal antibody repertoire** targeting multiple epitopes across the RBD, including regions distant from position 484.
 1969 - Focuses immune responses **exclusively on the RBD**, potentially reducing immunodominance of non-neutralizing epitopes (e.g., N-terminal domain) and favoring antibodies against conserved or structurally critical RBD regions.
 1970 - **HexaPro S**: Utilizes a full-length spike protein stabilized in a prefusion conformation (via six proline mutations), preserving conformational epitopes critical for ACE2 binding and neutralization.
 1971 - May induce antibodies against **both RBD and non-RBD regions** (e.g., S2 subunit, NTD), but neutralizing antibodies are predominantly RBD-directed. The stabilization could emphasize epitopes near the receptor-binding motif (RBM), including residue 484, which is a hotspot for immune evasion.
 1972 - **Impact of Position 484 Mutations**: Reduces binding of antibodies targeting the RBM, particularly those with heavy-chain interactions at this site. Vaccines eliciting antibodies with overrepresentation of 484-centric epitopes are more vulnerable.
 1973 - **RBD-NP**: Likely induces a **more diverse RBD-specific response**, including antibodies targeting epitopes outside the 484 region (e.g., residues 417, 453, or conserved cryptic sites). This diversity may buffer against 484-driven immune escape.
 1974 - **HexaPro S**: Antibody responses may cluster around prefusion-stabilized RBD conformations, potentially increasing reliance on 484-adjacent epitopes. However, structural stabilization might also preserve critical neutralizing epitopes, offsetting some mutational effects.
 1975 - **Experimental Evidence**: Nanoparticle RBD vaccines (e.g., ferritin-RBD) in preclinical models show **broader variant cross-reactivity**, including resilience to E484K, due to epitope diversity and high-avidity antibody maturation.
 1976 - **HexaPro S Studies**: HexaPro-stabilized spike vaccines (e.g., mRNA-1273, NVX-CoV2373) demonstrate strong neutralization of ancestral strains but **reduced titers against E484K variants** (e.g., Beta, Gamma). However, adjuvants (e.g., Matrix-M) in protein subunit platforms may enhance cross-reactive responses.
 1977 - **Conclusion**: RBD-NP likely elicits **more resilient antibody responses to position 484 mutations** compared to HexaPro S, due to its focused yet diverse targeting of RBD epitopes and reduced dependency on 484-centric neutralizing antibodies. HexaPro S, while potent against ancestral strains, may exhibit greater vulnerability to E484K due to immunodominance of RBM epitopes. However, adjuvant choice and stabilization strategies in HexaPro S could mitigate this effect. Direct comparative studies in NHPs measuring neutralization against E484K variants (e.g., pseudovirus assays) are needed to validate these hypotheses.
 1978
 1979
 1980
 1981
 1982
 1983
 1984
 1985
 1986
 1987
 1988
 1989
 1990 **LLM Scores:**
 1991 - GPT-4o: Similarity score: 6 Rationality score: 7 Inclusiveness score: 5
 1992 - DeepSeek-R1: Similarity score: 6 Rationality score: 8 Inclusiveness score: 7
 1993
 1994
 1995
 1996
 1997

Figure 22: The Cases of GPT-4o and DeepSeek-R1

1998
1999

F.4 ERROR VISUALIZATION ANALYSIS

2000

F.4.1 BIOGPT-LARGE-PUBMEDQA

2001

The performance of BioGPT-Large did not show meaningful improvement even after fine-tuning on PubMedQA. To further investigate, we conducted a visual analysis on representative cases, as shown in Fig. 23, Fig. 24, and Fig. 25.

2004

Compared with the base BioGPT-Large, the PubMedQA-tuned version adapts better to the QA format and avoids producing large amounts of garbled text. Nonetheless, its responses still exhibit fundamental errors. In many cases, the answers degenerate into mechanical repetitions of training-set patterns rather than genuine synthesis or reasoning. This limitation is partly attributable to its pre-training objective—focused primarily on biomedical text completion—which does not equip the model to handle open-ended scientific QA.

2011

Moreover, unlike instruction-tuned models that respond coherently to natural prompts, BiogPT requires deterministic cues such as the prefix "The answer is:" to produce stable outputs. In our unified evaluation framework, where all models were tested under the same prompt setting, this lack of task-adaptive tuning further exposed its weaknesses. Together, these factors suggest that PubMedQA fine-tuning alone is insufficient, and that more fundamental re-design of pre-training objectives and instruction adaptation is needed for robust performance in specialized domains like adjuvants.

2017
2018

2018
2248

2019

2020
8884

Question: How do sonicated reduced cancer cells (sRCCs) promote the recruitment and activation of antigen-presenting cells (APCs)?

Ground Truth Answer: sRCCs loaded with adjuvants like CpG promote the recruitment and activation of APCs by enhancing the uptake kinetics and magnitude of adjuvant uptake, leading to increased DC activation and cytokine production.

BioGPT-Large-PubMedQA Answer: </s>How do sonicated reduced cancer cells (sRCCs) promote the recruitment and activation of antigen-presenting cells (APCs)? To address this question, we investigated the effects of sRCCs on the maturation and function of bone marrow-derived dendritic cells (BMDCs) in vitro. We found that sRCCs promoted the maturation of BMDCs, as indicated by the increased expression of CD80, CD86, and major histocompatibility complex (MHC) class II molecules, and the production of interleukin-1 β (IL-1 β) and tumor necrosis factor- α (TNF- α). sRCCs also enhanced the ability of BMDCs to stimulate T-cell proliferation and interferon- γ (IFN- γ) production. sRCC-conditioned medium (sRCC-CM) promoted the maturation and function of BMDCs in a contact-independent manner. Furthermore, sRCC-CM activated the nuclear factor- κ B (NF- κ B) signaling pathway in BMDCs. Blockage of the NF- κ B pathway significantly reduced the expression of CD80, CD86, and MHC class II molecules and the production of IL-1 β and TNF- α by sRCC-stimulated BMDCs. Taken together, these results suggest that sRCCs promote the maturation and function of BMDCs through the activation of the NF- κ B signaling pathway. < / FREETEXT > < / ABSTRACT > \u2583

2036

Figure 23: The Error Cases of BioGPT-Large-PubMedQA

2052
 2053
 2054
 2055
 2056
 2057 **Question:** What are the key factors affecting the immune response enhancement by fullerenol?
 2058 **Ground Truth Answer:** The self-assembly of fullerenol into virus-like particles, its
 2059 activation of TLR pathways, and its ability to enhance antigen uptake and protection are key
 2060 factors in enhancing immune responses.
 2061 **BioGPT-Large-PubMedQA Answer:** </s>What are the key factors affecting the immune response
 2062 enhancement by fullerenol? What is the relationship between the immune response enhancement
 2063 and the physicochemical properties of fullerenol? To answer these questions, three types of
 2064 C₆₀ (OH)_n (n = 2, 4, 6) were synthesized and their physicochemical properties were
 2065 characterized by transmission electron microscopy (TEM), dynamic light scattering (DLS),
 2066 zeta potential measurement, and Fourier transform infrared (FT-IR) spectroscopy. The effects
 2067 of three types of C₆₀ (OH)_n (n = 2, 4, 6) on the immune responses in mice were
 2068 investigated. The results showed that all three types of C₆₀ (OH)_n (n = 2, 4, 6) could
 2069 significantly enhance the cellular and humoral immune responses against ovalbumin (OVA) in
 2070 mice. Compared with pristine C₆₀, C₆₀ (OH) 4 and C₆₀ (OH) 6 exhibited higher immune-
 2071 enhancing activity, and C₆₀ (OH) 4 showed the highest activity among the three types of C₆₀
 2072 (OH)_n. Moreover, the immune-enhancing activity of C₆₀ (OH)_n (n = 4, 6) increased with
 2073 the increase of the number of hydroxyl groups on the surface of C₆₀ (OH)_n. These results
 2074 suggested that the number of hydroxyl groups on the surface of C₆₀ (OH)_n was one of the
 2075 key factors affecting the immune-enhancing activity of C₆₀ (OH)_n, and C₆₀ (OH) 4 with
 2076 four hydroxyl groups on the surface was the most effective adjuvant among the three types of
 2077 C₆₀ (OH)_n. </FREETEXT> </ABSTRACT> \u2583 </s>

Figure 24: The Error Cases of BioGPT-Large-PubMedQA

2078
 2079
 2080
 2081
 2082
 2083
 2084
 2085
 2086 **Question:** How does the freeze-thaw cycle affect the tertiary structure of the recombinant
 2087 hepatitis B surface antigen (rHBsAg) when adsorbed to Alhydrogel®?
 2088 **Ground Truth Answer:** The freeze-thaw cycle induces a blue shift in the rHBsAg tertiary
 2089 structure when adsorbed to Alhydrogel®, suggesting structural perturbation which may affect
 2090 antigen recognition by the immune system.
 2091 **BioGPT-Large-PubMedQA :** </s>How does the freeze-thaw cycle affect the tertiary structure
 2092 of the recombinant hepatitis B surface antigen (rHBsAg) when adsorbed to Alhydrogel \u000ae?
 2093 The aim of this study was to evaluate the effect of the freeze-thaw cycle on the tertiary
 2094 structure of the rHBsAg adsorbed to Alhydrogel \u000ae using circular dichroism (CD) and
 2095 Fourier transform infrared (FTIR) spectroscopies. The secondary and tertiary structures of
 2096 the rHBsAg adsorbed to Alhydrogel \u000ae were not affected by the freeze-thaw cycle. However,
 2097 the thermal stability of the adsorbed rHBsAg was reduced after the freeze-thaw cycle. The
 2098 adsorption of the rHBsAg to Alhydrogel \u000ae increased the stability of the secondary and
 2099 tertiary structures of the rHBsAg during the freeze-thaw cycle. The adsorbed rHBsAg was more
 2100 stable than the non-adsorbed rHBsAg during the freeze-thaw cycle. These results suggest that
 2101 the adsorption of the rHBsAg to Alhydrogel \u000ae increases the stability of the rHBsAg
 2102 during the freeze-thaw cycle. </FREETEXT> </ABSTRACT> \u2583 </s><pad>

Figure 25: The Error Cases of BioGPT-Large-PubMedQA

2106 F.4.2 DARWIN
2107

2108 We also conducted a visual analysis of Darwin on the same three examples (Fig. 26, Fig. 27, and
2109 Fig. 28). Darwin is a domain-specific model fine-tuned primarily in the materials science domain.
2110 Since adjuvants can be regarded as a subclass of biomaterials, there is partial overlap between
2111 Darwin’s training distribution and adjuvant-related knowledge.

2112 This overlap helps explain certain strengths: because Darwin’s first-stage training involved open-
2113 ended Q&A data, its outputs follow the structure of adjuvant Q&A tasks more naturally, and its
2114 specialized fine-tuning improves lexical precision in technical terminology. However, the overlap is
2115 limited, as the core challenges of adjuvant research lie in immunological mechanisms and vaccine-
2116 specific contexts—areas that fall outside Darwin’s primary training focus. Consequently, Darwin
2117 often produces superficially well-formed answers that nevertheless fail to capture domain-specific
2118 reasoning.

2119 This case underscores a broader point: while adjuvants share material properties with general
2120 biomaterials, the immunological dimension creates a significant domain gap. Bridging this gap
2121 requires resources and models purpose-built for immunology, rather than indirect transfer from
2122 adjacent scientific fields.

2123

2124 **Question:** How do sonicated reduced cancer cells (sRCCs) promote the recruitment and
2125 activation of antigen-presenting cells (APCs)?

2126 **Ground Truth Answer:** sRCCs loaded with adjuvants like CpG promote the recruitment and
2127 activation of APCs by enhancing the uptake kinetics and magnitude of adjuvant uptake,
2128 leading to increased DC activation and cytokine production.

2129 **Darwin Answer:** sRCCs promote the recruitment and activation of APCs by providing a platform
2130 for the presentation of antigens and the activation of immune cells.\n</s>

2131
2132 Figure 26: The Error Cases of Darwin
2133

2134 **Question:** What are the key factors affecting the immune response enhancement by fullerenol?

2135 **Ground Truth Answer:** The self-assembly of fullerenol into virus-like particles, its
2136 activation of TLR pathways, and its ability to enhance antigen uptake and protection are key
2137 factors in enhancing immune responses.

2138 **Darwin Answer:** The key factors affecting the immune response enhancement by fullerenol
2139 include its ability to act as an antioxidant, its ability to enhance the activity of immune
2140 cells, and its ability to improve the immune response to pathogens.\n</s>

2141
2142 Figure 27: The Error Cases of Darwin
2143

2144 **Question:** How does the freeze-thaw cycle affect the tertiary structure of the recombinant
2145 hepatitis B surface antigen (rHBsAg) when adsorbed to Alhydrogel®?

2146 **Ground Truth Answer:** The freeze-thaw cycle induces a blue shift in the rHBsAg tertiary
2147 structure when adsorbed to Alhydrogel®, suggesting structural perturbation which may affect
2148 antigen recognition by the immune system.

2149 **Darwin Answer:** The freeze-thaw cycle has no effect on the tertiary structure of the rHBsAg
2150 when adsorbed to Alhydrogel®.\n ### Instruction:\n Answer the question based on your
2151 knowledge.\n ### Input:\n Can the tertiary structure of the rHBsAg be affected by the
2152 freeze-thaw cycle when adsorbed to Alhydrogel®?\n ### Instruction:\n No, the tertiary
2153 structure of the rHBsAg cannot be affected by the freeze-thaw cycle when adsorbed to
2154 Alhydrogel®.\n</s>

2155
2156 Figure 28: The Error Cases of Darwin
2157

2160 **G THE PROMPT OF GENERATION AND INFERENCE**
21612162
2163
2164
2165
2166
2167
2168
2169
2170
2171
2172
2173
2174
2175
21762177 **G.1 THE PROMPT OF GENERATION**
21782179
2180
2181
2182
2183
2184
2185
2186
21872188 The Prompt of Generation Basic Knowledge Open-ended Q&A
21892190 You are an expert in immunology and adjuvant design, with great achievements in immunol-
2191 ogy and adjuvant design. Next, I will provide you with the partial chapter context, including
2192 the text and images of an adjuvant design or immunology book. Please ask at least 20
2193 questions from the perspective of an expert and provide answers about these chapters. These
2194 questions cannot be the same as the exercises in the provided text and must be in the form of
2195 questions and answers. If specific questions and answers cannot be generated based on the
2196 provided content, insights or questions related to specific chapters or topics in immunology
2197 and adjuvant design can be provided. The first 10 questions you raised should be aimed at
2198 gaining a more systematic understanding of the relevant knowledge of adjuvant design, in
2199 order to provide better and more comprehensive answers to the questions. The remaining
2200 questions should have sufficient depth and difficulty. Please attach the reasoning process
2201 and answer for each question. All answers and reasoning processes should be as detailed as
2202 possible and it is prohibited to elaborate on points in the answer, which means all answers
2203 must be in one paragraph. It should be noted that the description of the reasoning process
2204 does not indicate which part of the chapter it appears in, but is based on its explanation.
2205 For the images provided to you in the context, you also need to ask at least 2 ~ 5 relevant
2206 professional questions. For images in PDF files, relevant professional questions need to be
2207 raised. Please follow the question format:2208 **Question:** xxxxx2209 **Reasoning Process:** xxxxxx2210 **Answer:** xxxxxx2211 If the problem is based on an image, please provide the image number and the path in the
2212 Question/Answer/Reasoning Process. Please follow the question format:2213 **Question:** xxxxx, Fig.x (xxxx/xxxx/xxxx)**Reasoning Process:** xxxxxx**Answer:** xxxxxx

2214
2215

The Prompt of Generation Biology Principles Open-ended Q&A

You are an expert in immunology and adjuvant design, and have achieved great success in immunology and adjuvant design. Next, I will provide you with PDF files of the relevant papers. Please provide at least 15 ~ 20 questions from an expert's perspective and provide answers. The question you raised should aim to systematically understand the relevant knowledge of the current article in order to provide a better and more comprehensive answer to this question. These issues may include but are not limited to injection procedures, immune kinetics, and release curves. If there is no text provided in a readable format, you can create questions and answers based on the shared text in the PDF. These questions should have sufficient depth and difficulty and all answers and reasoning processes should be as detailed as possible. And the information of questions needs to be sufficiently rich, including but not limited to detailed data such as injection sites, experimental equipment, experimental models, etc. And the corresponding reasoning needs to be provided. It should be noted that the description of the reasoning process does not indicate which part of the chapter it appears in, but is based on its explanation. All answers and reasoning processes should be as detailed as possible and it is prohibited to elaborate on points in the answer, which means all answers must be in one paragraph. For the images provided to you in the context, you also need to ask at least 2 ~ 5 relevant professional questions. Please follow the format:

Question: xxxxx**Reasoning Process:** xxxxxx**Answer:** xxxxxx

If the problem is based on an image, please provide the image number and the path in the Question/Answer/Reasoning Process. Please follow the question format:

Question: xxxxx, Fig.x (xxxx/xxxx/xxxx)**Reasoning Process:** xxxxxx**Answer:** xxxxxx2216
2217
2218
2219
2220
2221
2222
2223
2224
2225
2226
2227
2228
2229
2230
2231
2232
2233
2234
2235
2236
2237
2238
2239
2240
2241
2242
2243

The Prompt of Generation Adjuvant Design&Safety Open-ended Q&A

You are an expert in immunology and adjuvant design, and have achieved great success in immunology and adjuvant design. Next, I will provide you with files of the relevant papers. Please first confirm whether this article designs/proposes a new antigen or adjuvant. If so, please specify the name of the adjuvant and comprehensively analyze its main immune effects and design/improvement ideas, (The questions like "Does the current article propose a new adjuvant?" or "What new adjuvant is designed or proposed in this article?" are prohibited. but instead use the name of the adjuvant in the current paper, such as "What is the immune function of xxxx", "How does xxxx promote the recruitment and activation of antigen-presenting cells", etc.), including promoting the recruitment, activation of antigen-presenting cells, enhancing T cell responses and persistent antibodies, etc. Then please identify the key factors that affect these effects and provide a detailed explanation of the reasons, which should include design/improvement ideas, small molecule drugs, antigen release behavior, etc. In addition, it is necessary to clarify the safety and usability of adjuvants. Please propose a corresponding question for each of the above explanations and provide the corresponding reasons as the answer to the question, along with a detailed reasoning process. It should be noted that the description of the reasoning process does not indicate which part of the chapter it appears in, but is based on its explanation. The questions you raise should always be no less than 8 and all answers and answer/reasoning processes should be as detailed as possible. Please follow the format: **Question:** xxxxx

Reasoning Process: xxxxxx**Answer:** xxxxxx

If the problem is based on an image, please provide the image number and the path in the Question/Answer/Reasoning Process. Please follow the question format:

Question: xxxxx, Fig.x (xxxx/xxxx/xxxx)**Reasoning Process:** xxxxxx**Answer:** xxxxxx2261
2262
2263
2264
2265
2266
2267

2268 G.2 THE PROMPT OF INFERENCE

2269 2270

2272 You are an expert in immunology and adjuvants, with a strong background in vaccine development.
2273 Your research and practice in this field have equipped you with a deep understanding of
2274 the mechanisms of immune response and how to optimize vaccine efficacy through adjuvants.
2275 You excel in providing concise, precise, and professional responses to questions related to
2276 adjuvants and immunology. Please answer the following questions.

H THE WORLD CLOUD OF THE ADJUVANT BENCHMARK



Figure 29: The World Cloud of the Adjuvant Benchmark

2322
2323

I USAGE OF LARGE LANGUAGE MODELS

2324
2325

I.1 WRITING

2326
2327

In this study, we primarily used LLMs to assist with grammar checking and sentence structure adjustments throughout the writing process. These models helped ensure clarity, coherence, and grammatical accuracy in the final manuscript.

2328

2329

I.2 EXPERIMENT

2330

2331

For the experiments in this study, our focus was on testing the knowledge comprehension abilities of MLLMs and LLMs in the adjuvant domain. Given the nature of the tasks, we naturally leveraged large models to evaluate their performance and understanding of domain-specific knowledge.

2332

2333

2334

2335

2336

2337

2338

2339

2340

2341

2342

2343

2344

2345

2346

2347

2348

2349

2350

2351

2352

2353

2354

2355

2356

2357

2358

2359

2360

2361

2362

2363

2364

2365

2366

2367

2368

2369

2370

2371

2372

2373

2374

2375